Ted Barnes
Physics Div. ORNL,
Dept. of Physics, U.Tenn.

The Status of Exotics*

1) *Color singlets and QCD exotica*
2) *Early history: states, spectrum and decays*
3) *LGT predictions*
4) *Current expt. candidates*

*Specifically, hybrids (quark+gluon excitations).

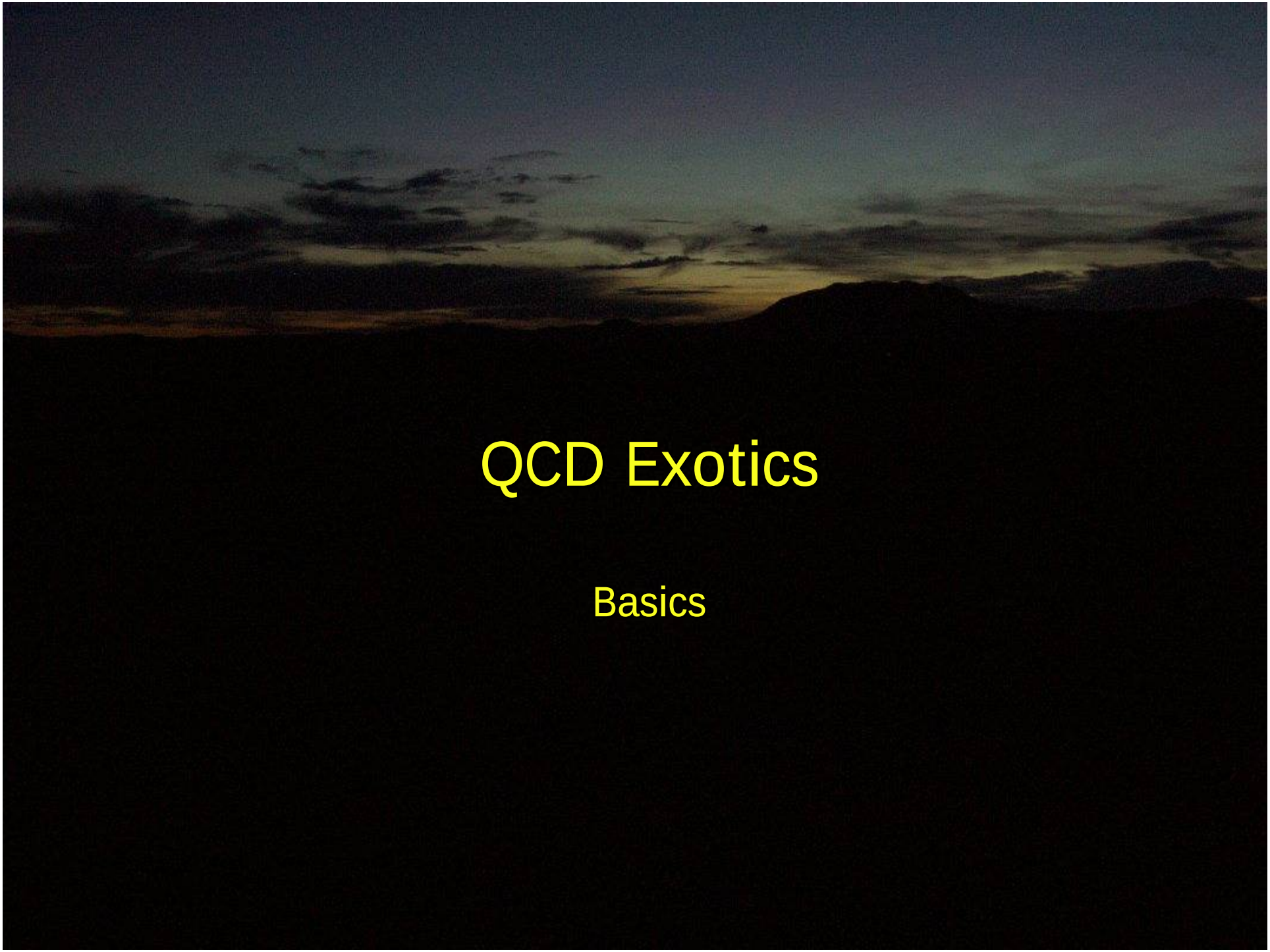
QCD Exotics
Basics

Color singlets and QCD exotica
"confinement happens".

LGT simulation showing the QCD flux tube

Q Q̄

R = 1.2 [fm]

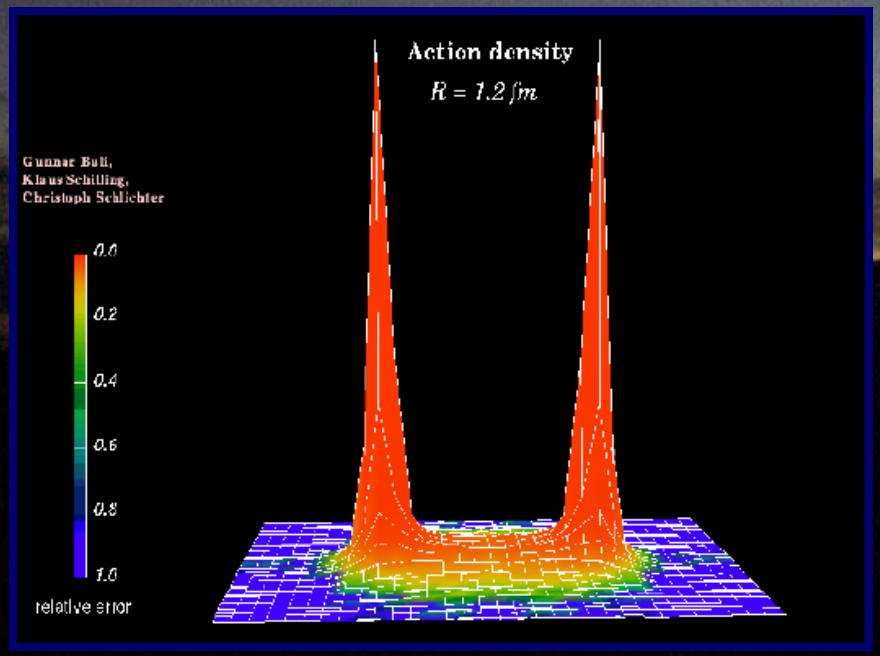

QCD flux tube (LGT, G.Bali et al.; hep-ph/010032)

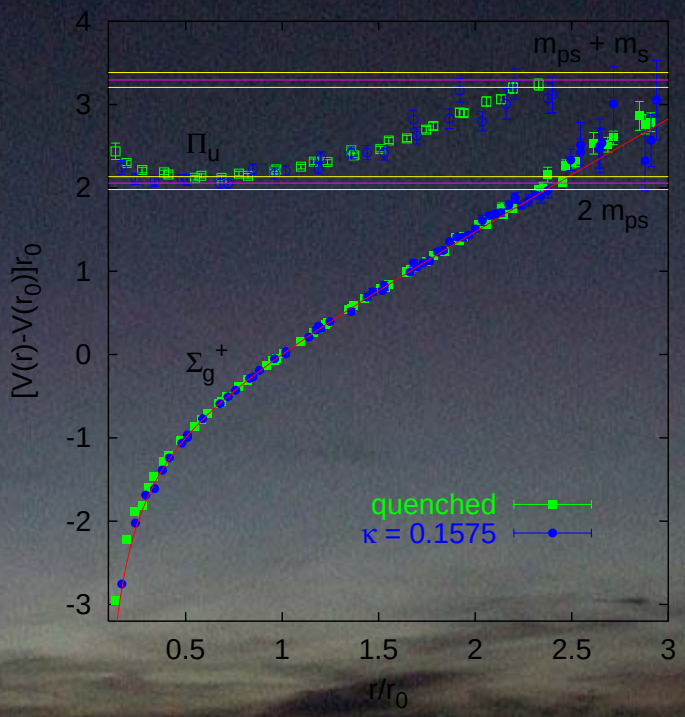

"funnel-shaped" $V_{Q\bar{Q}}(R)$

Coul. (OGE)

linear conft. (str. tens. = 16 T)

Physically allowed hadron states (color singlets)

$q\bar{q}$

q^3

Conventional quark model
mesons and baryons.

100s of e.g.s

$(q^3)^n$, $(q\bar{q})(q\bar{q})$, $(q\bar{q})(q^3)$,…

Basis state mixing may be
very important in some sectors.

nuclei / molecules

"exotica" :

ca. 10^6 e.g.s of $(q^3)^n$, maybe 1-3 others
X(3872) = DD!*

g^2, g^3,…

qqg, q^3g,…

$(q^2\bar{q}^2)^n$, $(q^2\bar{q}^2)q(q\bar{q})$, $(q^4\bar{q}^4)$,…

glueballs

maybe 1 e.g.

hybrids

maybe 1-3 e.g.s

multiquarks

controversial
e.g. $\Theta(1540)$

$q\bar{q}$ *mesons*; states and spectrum.

The nonrelativistic quark model treats conventional mesons as $q\bar{q}$ bound states.

Since each quark has spin-1/2, the total spin is

$$S_{q\bar{q}}^{tot.} = \tfrac{1}{2} \times \tfrac{1}{2} = 1 + 0$$

Combining this with orbital angular momentum $L_{q\bar{q}}$ gives states of total

$$J_{q\bar{q}} = L_{q\bar{q}} \qquad \textit{spin singlets}$$

$$J_{q\bar{q}} = L_{q\bar{q}}+1,\ L_{q\bar{q}},\ L_{q\bar{q}}-1 \qquad \textit{spin triplets}$$

Allowed $q\bar{q}$ quantum numbers:

Spatial parity $P_{q\bar{q}} = (-1)^{(L+1)}$ C-parity $C_{q\bar{q}} = (-1)^{(L+S)}$

(both established by observed decay modes, X -> even π^os -> PC=(++).)

The complete list of allowed $q\bar{q}$ J^{PC} quantum numbers has gaps!

The J^{PC} forbidden to $q\bar{q}$ are called "J^{PC}-exotic quantum numbers".

Exotic $J^{PC} = 0^{--}; 0^{+-}, 1^{-+}, 2^{+-}, 3^{-+}$ ...

If you find a resonance with exotic J^{PC},
you are certainly beyond the naive $q\bar{q}$ quark model.

Plausible J^{PC}-exotic candidates =
hybrids, glueballs (high mass), maybe multiquarks (fall-apart decays).

Charmonium (cc̄)

A nice example of a QQ̄ spectrum.
Expt. states (blue) are shown with the usual L classification.

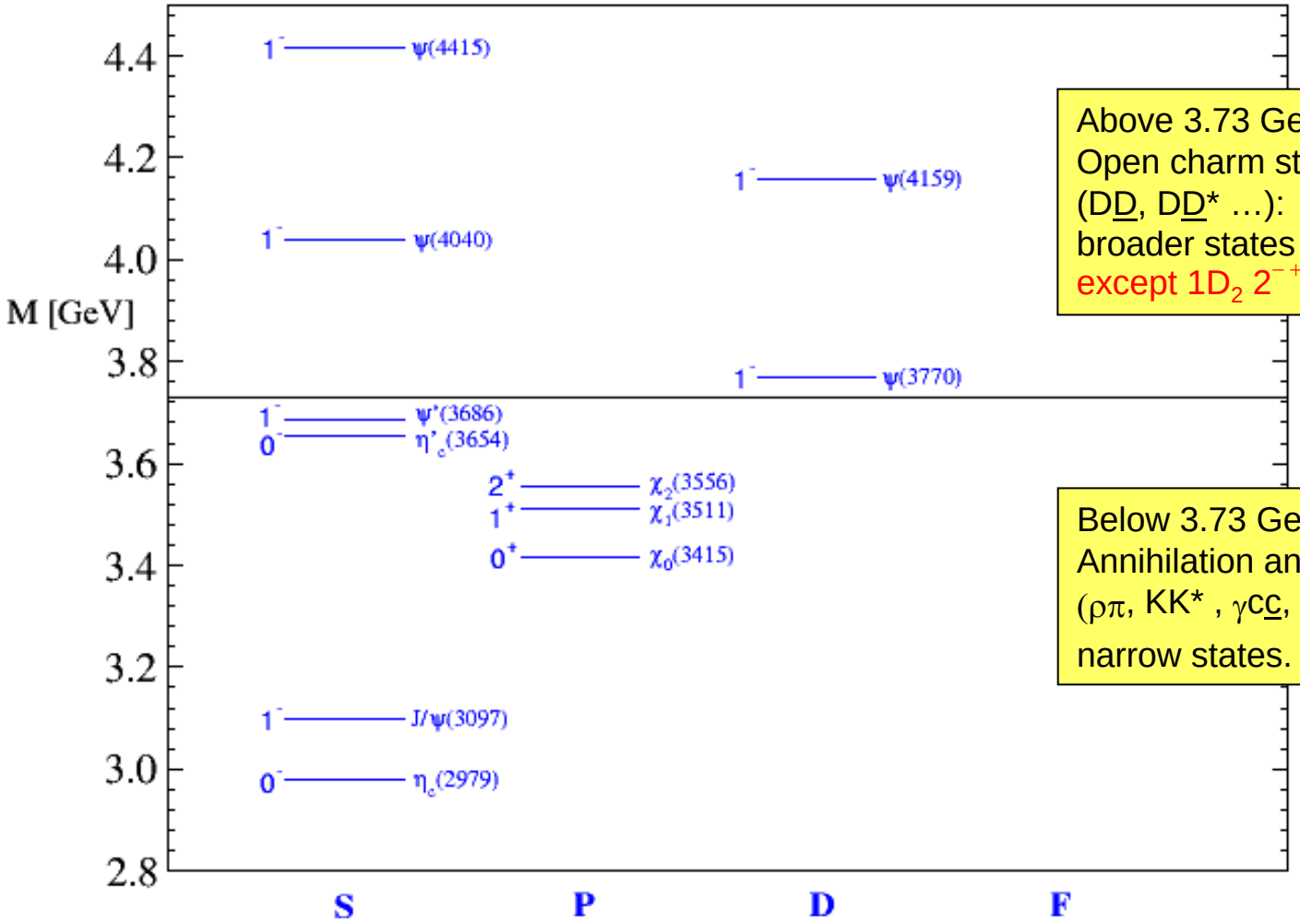

Above 3.73 GeV:
Open charm strong decays
(DD̄, DD̄* …):
broader states
except $1D_2$ 2^{-+}, 2^{--}

3.73 GeV

Below 3.73 GeV:
Annihilation and EM decays.
($\rho\pi$, KK* , $\gamma c\bar{c}$, $\gamma\gamma$, $\ell^+\ell^-$..):
narrow states.

Fitted and predicted cc̄ spectrum

Coulomb (OGE) + linear scalar conft. potential model

blue = expt, red = theory.

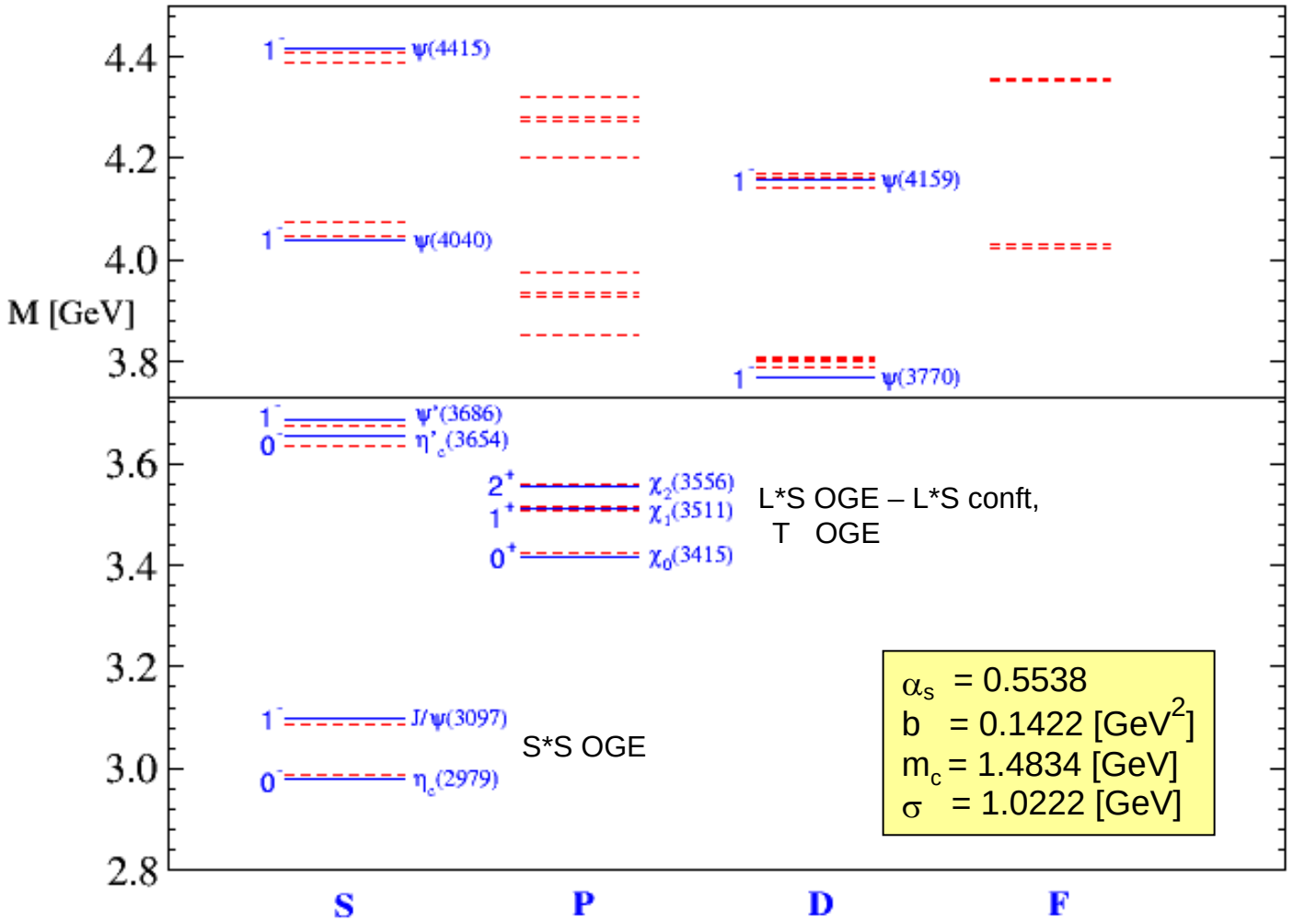

α_s = 0.5538
b = 0.1422 [GeV^2]
m_c = 1.4834 [GeV]
σ = 1.0222 [GeV]


Hybrid Mesons
Spectrum

The earliest hybrid spectrum calculations used the bag model and QCD sum rules.

Among the 1st bag model refs:
T.Barnes and F.E.Close, PLB123, 89 (1983), NPB224, 241 (1983); TB PhD (Caltech, 1977).
M.Chanowitz and S.R.Sharpe, NPB222, 211 (1983).

$$(q\bar{q})_{1^-,0^-} \otimes g_{1^+} \to 0^{-+}, 1^{-+}, 2^{-+}; 1^{--},$$

$$\mathrm{TM}(1^-) \simeq \mathrm{TE}(1^+) + 0.5\ \mathrm{GeV}.$$

$$|q\bar{q}g\rangle = \sum_{a=1}^{8} \sqrt{\tfrac{1}{8}}\,|q\bar{q}\rangle_a |g\rangle_a,$$

J^{PC} exotics

This multiplet was split by pQCD effects, e.g. :

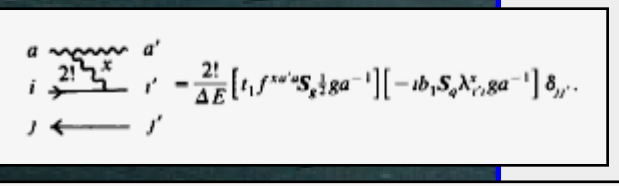

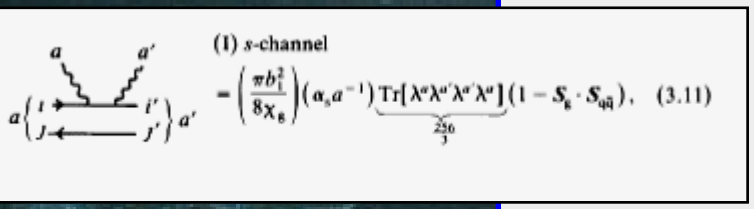

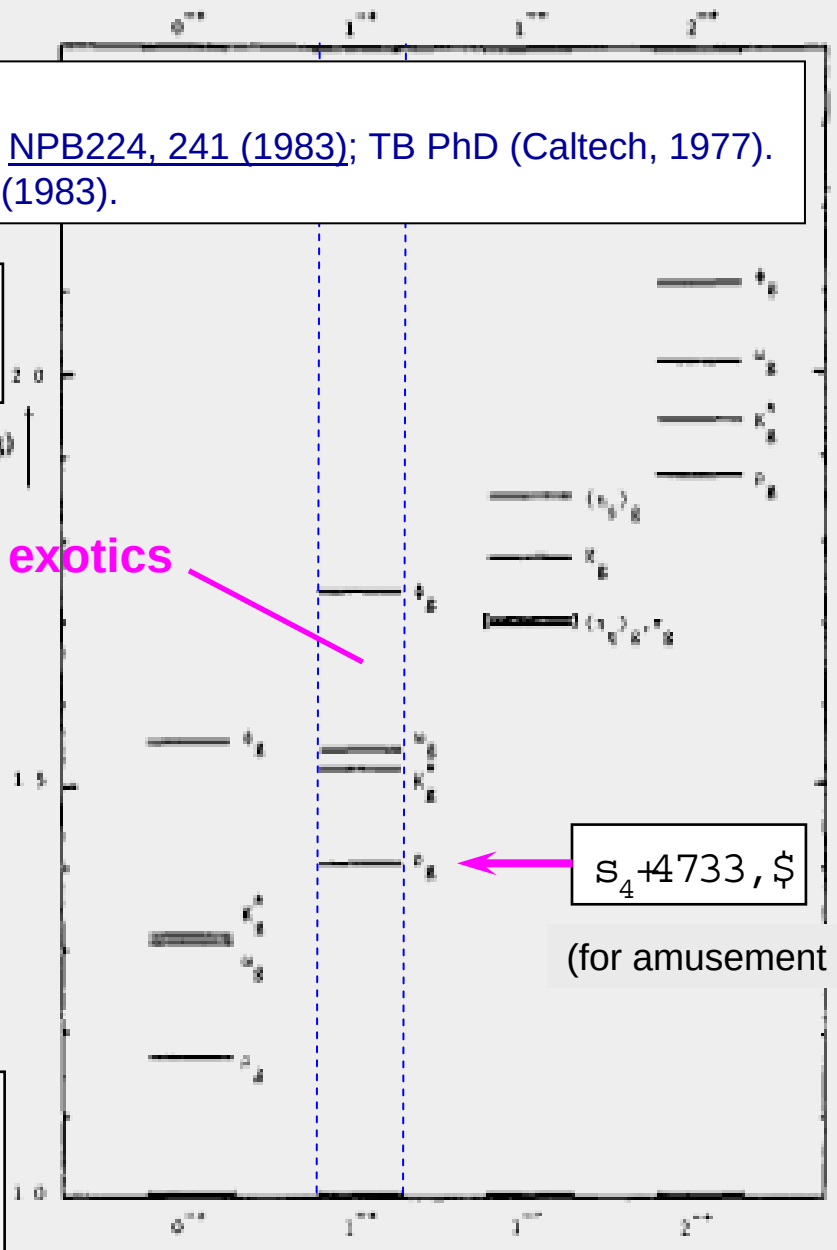

s_4+4733,$

(for amusement only)

Fig. 1. Hybrid meson masses. Parameters are $a = 6\ \mathrm{GeV}^{-1}$, $\alpha_s = 2.2$, thus gives $E_0 = 1.52$ GeV.

Refs. in hep-ph/9501405, PRD52, 5242 (1995).

TABLE I. Predicted 1^{-+} Hybrid Masses.

state	mass (GeV)	model	Ref.
$H_{u,d}$	1.3-1.8	bag model	[19]
	1.8-2.0	flux tube model	[11–14]
	2.1-2.5	QCD sum rules (most after 1984)	[26–28]
H_c	$\approx$ 3.9	adiabatic bag model	[20]
	4.2-4.5	flux tube model	[12–14]
	4.1-5.3	QCD sum rules (most after 1984)	[26–28]
	4.19(3) $\pm$ sys.	HQLGT	[23]
H_b	10.49(20)	adiabatic bag model	[20]
	10.8-11.1	flux tube model	[12–14]
	10.6-11.2	QCD sum rules (most after 1984)	[26–28]
	10.81(3) $\pm$ sys.	HQLGT	[23]

(J^{PC} = 3^{0-}/3^{0+}/4^{0-}/4^{0+}/5^{0-}/5^{0+}>4^{--}/4^{00}) ® flavor 9 = ***72 states***, 1st H multiplet!

N.Isgur, R.Kokoski and J.Paton, PRL 54, 869 (1985).

LGT spectrum calculations

Approach:

1. Choose an operator $J^{\dagger}$ that couples to the state of interest (correct quantum numbers) when operating on the vacuum state

$$\langle \text{state} | J^{\dagger} | 0 \rangle \neq 0$$

2. Use Monte-Carlo techniques to evaluate the imaginary-time correlation function

$$\int d^3x \ \langle 0 | J(x,\tau) J^{\dagger}(0,0) | 0 \rangle$$

At large τ this decays exponentially as $\exp(-M_{state}\tau)$, where M_{state} is the mass of the lightest state with these quantum numbers.

Complication: usually quenched approx, neglects closed quark loops, assumes stable hadrons. (Decays make the lightest I=1, $J^{PC} = 4^{0\,0}$ system created by $J^{\dagger}_{\bar{q}q} = \bar{s}s$, not $\rho(770)$.)

LGT spectrum calculations

J.N. Hedditch et al, hep-lat/0402016

Some examples of local operators J for conventional and exotic mesons:

1^{++}	1^{+-}	1^{-+}	1^{--}
$-i\bar{q}^a\gamma_5\gamma_j q^a$	$-i\bar{q}^a\gamma_5\gamma_4\gamma_j q^a$	$\bar{q}^a\gamma_4 E_j^{ab} q^b$	$-i\bar{q}^a\gamma_j q^a$
$i\bar{q}^a\gamma_4 B_j^{ab} q^b$	$i\bar{q}^a B_j^{ab} q^b$	$-\epsilon_{jkl}\bar{q}^a\gamma_k B_l^{ab} q^b$	$\bar{q}^a E_j^{ab} q^b$
$i\epsilon_{jkl}\bar{q}^a\gamma_k E_l^{ab} q^b$	$\bar{q}^a\gamma_5 E_j^{ab} q^b$	$\epsilon_{jkl}\bar{q}^a\gamma_4\gamma_k B_l^{ab} q^b$	$-i\bar{q}^a\gamma_5 B_j^{ab} q^b$
$i\epsilon_{jkl}\bar{q}^a\gamma_k\gamma_4 E_l^{ab} q^b$	$\bar{q}^a\gamma_5\gamma_4 E_j^{ab} q^b$	$-i\epsilon_{jkl}\bar{q}^a\gamma_5\gamma_4\gamma_k E_l^{ab} q^b$	$i\bar{q}^a\gamma_4\gamma_5 B_j^{ab} q^b$

J^{PC} exotic

Note that true **exotic** states (**1^{0} .** channel) can only be made from **qGq** operators.

States in the other (nonexotic) channels can be excited by **qq** or **qGq** operators (the latter couple to the hybrid components of conventional mesons).

Many useful cross-checks: the same mass M_{state} should follow from any operator pair in the same channel.

A summary of LGT 1^{0-} exotic hybrid masses.

X.Q.Luo and Z.H.Mei, hep-lat/0209049,
Nucl. Phys. Proc. Suppl. 119 (2003) 263.

nn - H

Light $1^{-+}\bar{q}qg$ (GeV)	Method	Ref.
1.97(9)(30)	Isotropic $S_g(\mathrm{W}) + S_q(\mathrm{W})$	MILC97[1]
1.87(20)	Isotropic $S_g^{\mathrm{TI}}(\mathrm{W}) + S_q^{\mathrm{TI}}(\mathrm{SW})$	UKQCD97[2]
2.11(10)	Isotropic $S_g^{\mathrm{TI}}(\mathrm{W}) + S_q^{\mathrm{TI}}(\mathrm{SW})$	MILC99[3]
2.013(26)(71)	Anisotropic $S_g^{\mathrm{TI}}(1\times1+2\times1) + S_q^{\mathrm{TI}}(\mathrm{SW})$	**ZSU (this work)**

cc - H

$1^{-+}\bar{q}qg$ (GeV)	Method	Ref.
4.390 (80) (200)	Isotropic $S_g(\mathrm{W}) + S_q(\mathrm{W})$	MILC97[1]
4.369 (37) (99)	Anisotropic $S_g^{\mathrm{TI}}(1\times1+2\times1) + S_q^{\mathrm{TI}}(\mathrm{SW})$	**ZSU (this work)**

$1^{-+}\bar{c}cg$ -1S $\bar{c}c$ splitting (GeV)	Method	Ref.
1.34(8)(20)	Isotropic $S_g(\mathrm{W}) + S_q(\mathrm{W})$	MILC97[1]
1.22(15)	Isotropic $S_g^{\mathrm{TI}}(\mathrm{W}) + S_q^{\mathrm{TI}}(\mathrm{SW})$	MILC99[3]
1.323(13)	Anisotropic $S_g^{\mathrm{TI}}(\mathrm{W}) + S_q^{\mathrm{TI}}(\mathrm{NRQCD})$	CP-PACS99[4]
1.19	Isotropic $S_g^{\mathrm{TI}}(1\times1+2\times1) + S_q^{\mathrm{TI}}(\mathrm{LBO})$	JKM99[5]
1.302(37)(99)	Anisotropic $S_g^{\mathrm{TI}}(1\times1+2\times1) + S_q^{\mathrm{TI}}(\mathrm{SW})$	**ZSU (this work)**

Table 1
Predictions for the masses of hybrid mesons. Abbreviations: W for Wilson, $1\times1+2\times1$ for the plaquette terms plus the rectangle terms, SW for Sheikholeslami-Wohlert (Clover), TI for tadpole-improved, NRQCD for non-relativistic QCD, and LBO for leading Born-Oppenheimer.

cc̄ from LGT

A LGT e.g.: X.Liao and T.Manke, hep-lat/0210030 (quenched – no decay loops) Broadly consistent with the cc̄ potential model spectrum. No radiative or strong decay predictions yet.

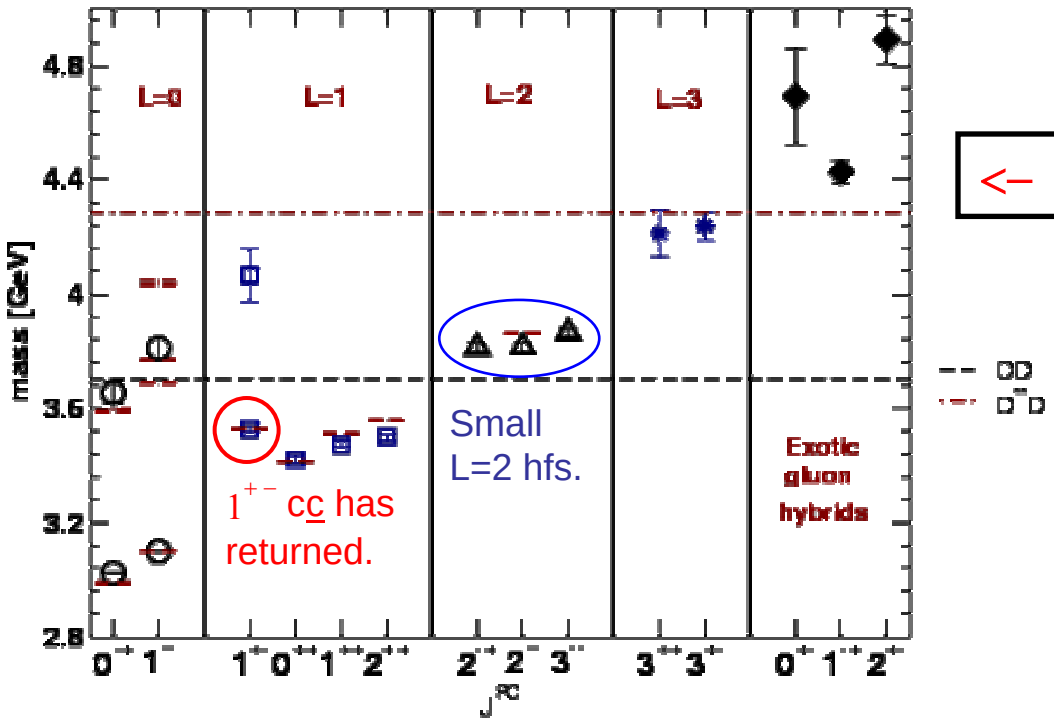

FIG. 1. Quenched charmonium spectrum. The experimental values are shown as short horizontal lines. The long horizontal dashed lines mark the $D\bar{D}$ and $D^{**}D$ thresholds. The mesons (please refer to appendix B 2 for our naming convention) plotted are $\pi(0^{-+})$, $\rho(1^{--})$, $b_1(1^{+-})$, $\rho \times \nabla A_1(0^{++})$, $\rho \times \nabla T_1(1^{++})$, $\rho \times \nabla T_2(2^{++})$, $\pi \times D T_2(2^{-+})$, $\rho \times D T_2(2^{--})$, $\rho \times D A_2(3^{--})$, $a_1 \times D A_2(3^{++})$, $b_1 \times D A_2(3^{+-})$, $a_1 \times B A_1(0^{+-})$, $\rho \times B T_1(1^{-+})$, and $a_1 \times B T_2(2^{+-})$. Some of the low-lying meson [$\pi(0^{-+})$, $\rho(1^{--})$, $b_1(1^{+-})$] are taken from Columbia group's previous work [18]. The lattice scale is set by the $^1P_1 - 1S$ splitting. The numerical values are listed in table II.

<- 1^{-+} exotic cc̄-H at 4.4 GeV

n.b.
$n_f = 0$ is quenched.

LGT spectrum calculations (recent devs.)

J.N. Hedditch et al, hep-lat/0402016

Confirmation of equal LGT "qq meson" masses using **q̲q̲** ***or*** **q̲Gq̲** sources.

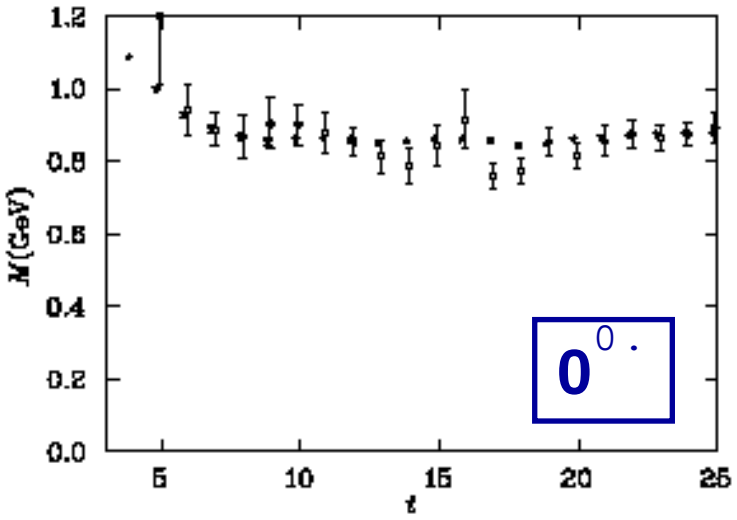

Figure 2. Effective mass plot for correlation functions of the standard pion interpolator $\bar{q}^a\gamma_5 q^a$ and the hybrid pion interpolator $\bar{q}^a\gamma_j B_j^{ab} q^b$.

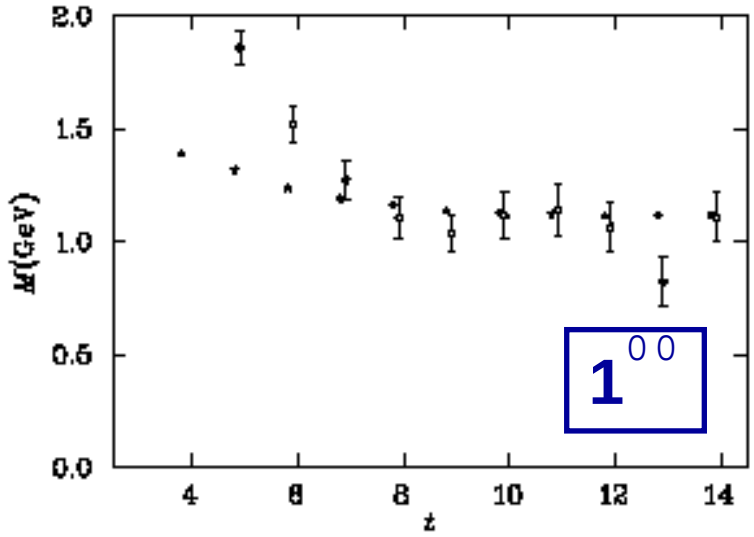

Figure 4. Effective mass plot for correlation functions of the standardρ-meson interpolator $\bar{q}^a\gamma_j q^a$ and the hybrid ρ interpolator $\bar{q}^a\gamma_4\gamma_5 B_j^{ab} q^b$.

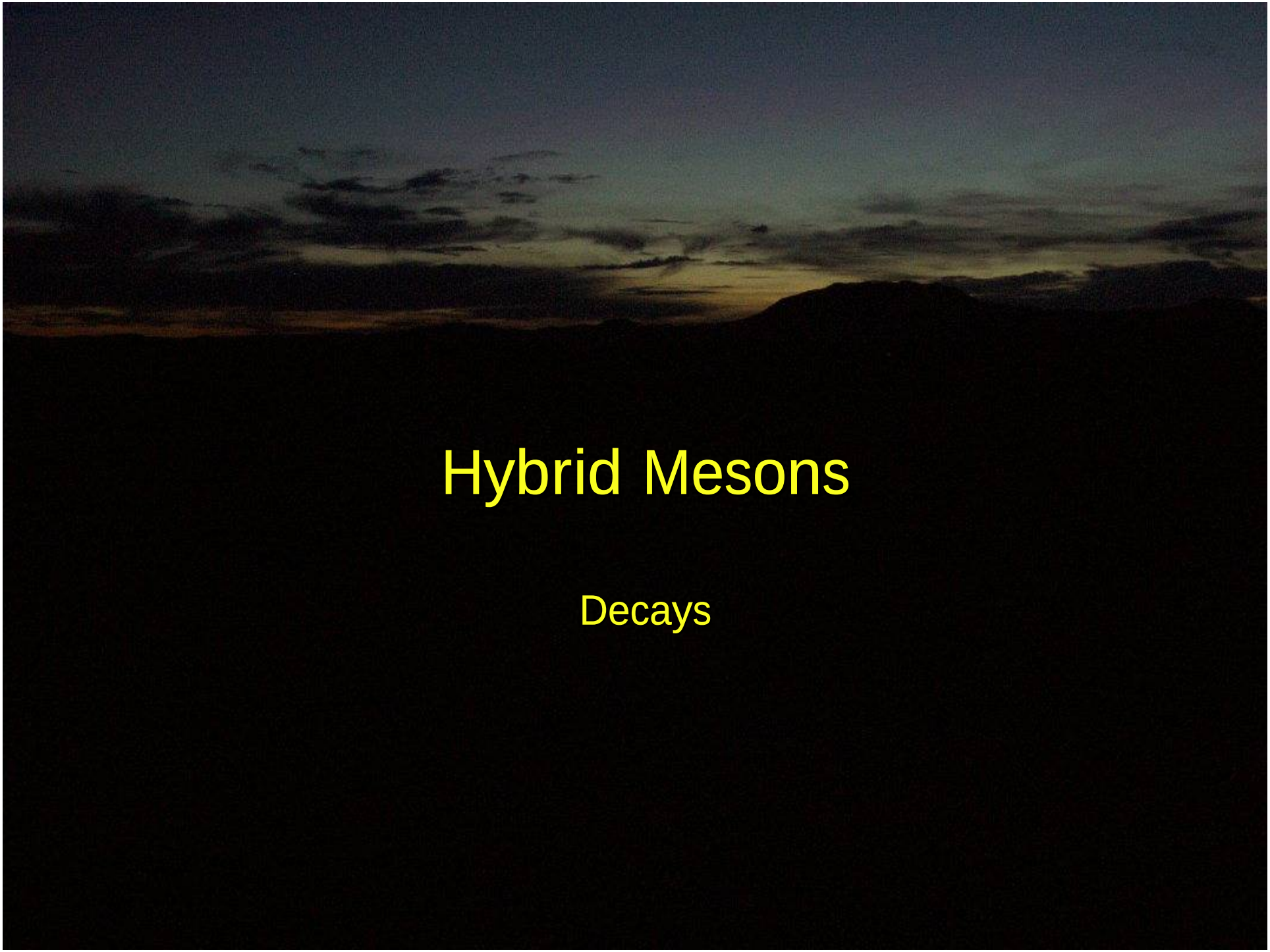
Hybrid Mesons
Decays

Hybrid Decays (light u,d,s quarks, f.-t. model)

Gluonic Excitations Of Mesons: Why They Are Missing And Where To Find Them
N.Isgur, R.Kokoski and J.Paton, PRL 54, 869 (1985).

Considers J^{PC}-exotic hybrids ($0^{+-}, 1^{-+}, 2^{+-}$) in the lightest f.-t. multiplet.
S+P decay modes dominant in f.-t. decay model.
π_1 -> $b_1\pi$ a nice case for experiment. $\pi\rho$, $\pi\eta$, $\pi\eta'$ etc should be small.

The Production and Decay of Hybrid Mesons by Flux-Tube Breaking
F.E.Close and P.R.Page, NPB443, 233 (1995). "IKP-2"

Confirms prev. results and also considers nonexotics ($0^{-+}, 1^{+-}, 2^{-+}, 1^{++}, 1^{--}$) in the lightest f.-t. multiplet. Some special cases of nonexotics predicted to be rather narrow if M_H = 1.6 GeV; extra ω and π_2 notable.

The f.-t. hybrid π_2 decays strongly to $b_1\pi$ in the f.-t. decay model.

Hybrid Meson Decays: flux-tube model

N.Isgur, R.Kokoski and J.Paton, PRL54, 869 (1985).

Gluonic Excitations of Mesons:
Why They Are Missing and Where to Find Them.

$H_{l=1} \rightarrow S+P$

TABLE I. The dominant decays of the low-lying exotic meson hybrids.

Hybrid state[a]	J^{PC}	(Decay mode)$_{L \text{ of decay}}$	Partial width (MeV)
x_2^{+-} (1900)	2^{++}	$(\pi A_2)_P$	450
		$(\pi A_1)_P$	100
		$(\pi H)_P$	150
y_2^{+-} (1900)	2^{+-}	$(\pi B)_P$	500
z_2^{+-} (2100)	2^{+-}	$[\bar{K}K^*(1420)+\text{c.c.}]_P$	250
		$(\bar{K}Q_2+\text{c.c.})_P$	200
x_1^{-+} (1900)	1^{-+}	$(\pi B)_{S,D}$	100,30
		$(\pi D)_{S,D}$	30,20
y_1^{-+} (1900)	1^{-+}	$(\pi A_1)_{S,D}$	100,70
		$[\pi\pi(1300)]_P$	100
		$(\bar{K}Q_2+\text{c.c.})_S$	~ 100
z_1^{-+} (2100)		$(\bar{K}Q_1+\text{c.c.})_D$	80
		$(\bar{K}Q_2+\text{c.c.})_S$	250
		$[\bar{K}K(1400)+\text{c.c.}]_P$	30
x_0^{+-} (1900)	0^{++}	$(\pi A_1)_P$	800
		$(\pi H)_P$	100
		$[\pi\pi(1300)]_S$	900
y_0^{+-} (1900)	0^{+-}	$(\pi B)_P$	250
z_0^{+-} (2100)	0^{+-}	$(\bar{K}Q_1+\text{c.c.})_P$	800
		$(\bar{K}Q_2+\text{c.c.})_P$	50
		$[\bar{K}K(1400)+\text{c.c.}]_S$	800

[a] x, y, and z denote the flavor states $(1/\sqrt{2})(u\bar{u}-d\bar{d})$, $(1/\sqrt{2})(u\bar{u}+d\bar{d})$, and $s\bar{s}$. The subscript on a state is J; the superscripts are P and C_n.

$\pi_1 \rightarrow b_1\pi, f_1\pi$

I = 1

$\pi_2(2000)$ **hybrid;** $b_1\pi$ **mode**

narrow nonexotic hybrids

A	B,C	L	Γ	A	B,C	L	Γ	A	B,C	L	Γ
2^{-+}	$f_2(1270)\pi$	S	40	1^{+-}	$a_2(1320)\pi$	P	175	1^{-+}	$f_1(1285)\pi$	S	40
		D	20		$a_1(1260)\pi$	P	90			D	20
	$b_1(1235)\pi$	D	40		$h_1(1170)\pi$	P	175		$b_1(1235)\pi$	S	150
	$a_2(1320)\eta$	S	~ 40		$b_1(1235)\eta$	P	150			D	20
	$K_2^*(1430)K$	S	~ 30		$K_2^*(1430)K$	P	60		$a_1(1260)\eta$	S	50
2^{+-}	$a_2(1320)\pi$	P	200		$K_1(1270)K$	P	250		$K_1(1270)K$	S	20
	$a_1(1260)\pi$	P	70		$K_0^*(1430)K$	P	70		$K_1(1400)K$	S	~ 125
	$h_1(1170)\pi$	P	90	1^{++}	$f_2(1270)\pi$	P	175	0^{-+}	$f_2(1270)\pi$	D	20
	$b_1(1235)\eta$	P	~ 15		$f_1(1285)\pi$	P	150		$f_0(1300)\pi$	S	~ 150
0^{+-}	$a_1(1260)\pi$	P	700		$f_0(1300)\pi$	P	~ 20		$K_0^*(1430)K$	S	~ 200
	$h_1(1170)\pi$	P	125		$a_2(1320)\eta$	P	50	1^{--}	$a_2(1320)\pi$	D	50
	$b_1(1235)\eta$	P	80		$a_1(1260)\eta$	P	90		$a_1(1260)\pi$	S	150
	$K_1(1270)K$	P	600		$K_2^*(1430)K$	P	~ 20			D	20
	$K_1(1400)K$	P	150		$K_1(1270)K$	P	40		$K_1(1270)K$	S	40
					$K_1(1400)K$	P	~ 20		$K_1(1400)K$	S	~ 60

$4\#^{0^{-}}$ exotics

Close and Page: ***some notable nonexotic hybrids in the flux tube model***

I = 0

$\eta_2(2000)$ **hybrid**

$\omega(2000)$ **hybrid**

A	B,C	L	Γ	A	B,C	L	Γ	A	B,C	L	Γ
2^{-+}	$a_2(1320)\pi$	S	125	2^{+-}	$b_1(1235)\pi$	P	250	1^{++}	$a_2(1320)\pi$	P	500
		D	60		$h_1(1170)\eta$	P	30		$a_1(1260)\pi$	P	450
	$f_2(1270)\eta$	S	~ 50	0^{+-}	$b_1(1235)\pi$	P	300		$f_2(1270)\eta$	P	70
	$K_2^*(1430)K$	S	~ 30		$h_1(1170)\eta$	P	90		$f_1(1285)\eta$	P	60
1^{+-}	$b_1(1235)\pi$	P	500		$K_1(1270)K$	P	600		$K_2^*(1430)K$	P	~ 20
	$h_1(1170)\eta$	P	175		$K_1(1400)K$	P	150		$K_1(1270)K$	P	40
	$K_2^*(1430)K$	P	60	1^{-+}	$a_1(1260)\pi$	S	100		$K_1(1400)K$	P	~ 20
	$K_1(1270)K$	P	250			D	70	0^{-+}	$a_2(1320)\pi$	D	60
	$K_0^*(1430)K$	P	70		$f_1(1285)\eta$	S	50		$f_0(1300)\eta$	S	~ 200
1^{--}	$K_1(1270)K$	S	40		$K_1(1270)K$	S	20		$K_0^*(1430)K$	S	~ 200
	$K_1(1400)K$	S	60		$K_1(1400)K$	S	~ 125				

… and much narrower if M ≲ 1750 MeV !

LGT studies of strong decays

"The two ways to learn about hadrons are lattice gauge theory and experiment." *-Sanderling report (draft), 2000*

LGT has been applied to strong decays of glueballs, conventional light mesons, and heavy-quark hybrids.

The results are all "to be confirmed", and some LGT practitioners are skeptical.

Nonetheless here are some references and results:

J #ghfd|v

Strong M_{Ps} dependence of the G-PsPs coupling reported in an early LGT study. This complicates nn-ss-G mixing angle determinations from $f_0(1500)$ decays that assume flavor-blind G decay amplitudes.

J.Sexton, A.Vaccarino and D.Weingarten,
NPB (PS) 42, 279 (**1995**);
PRL75, 4563 (**1995**).

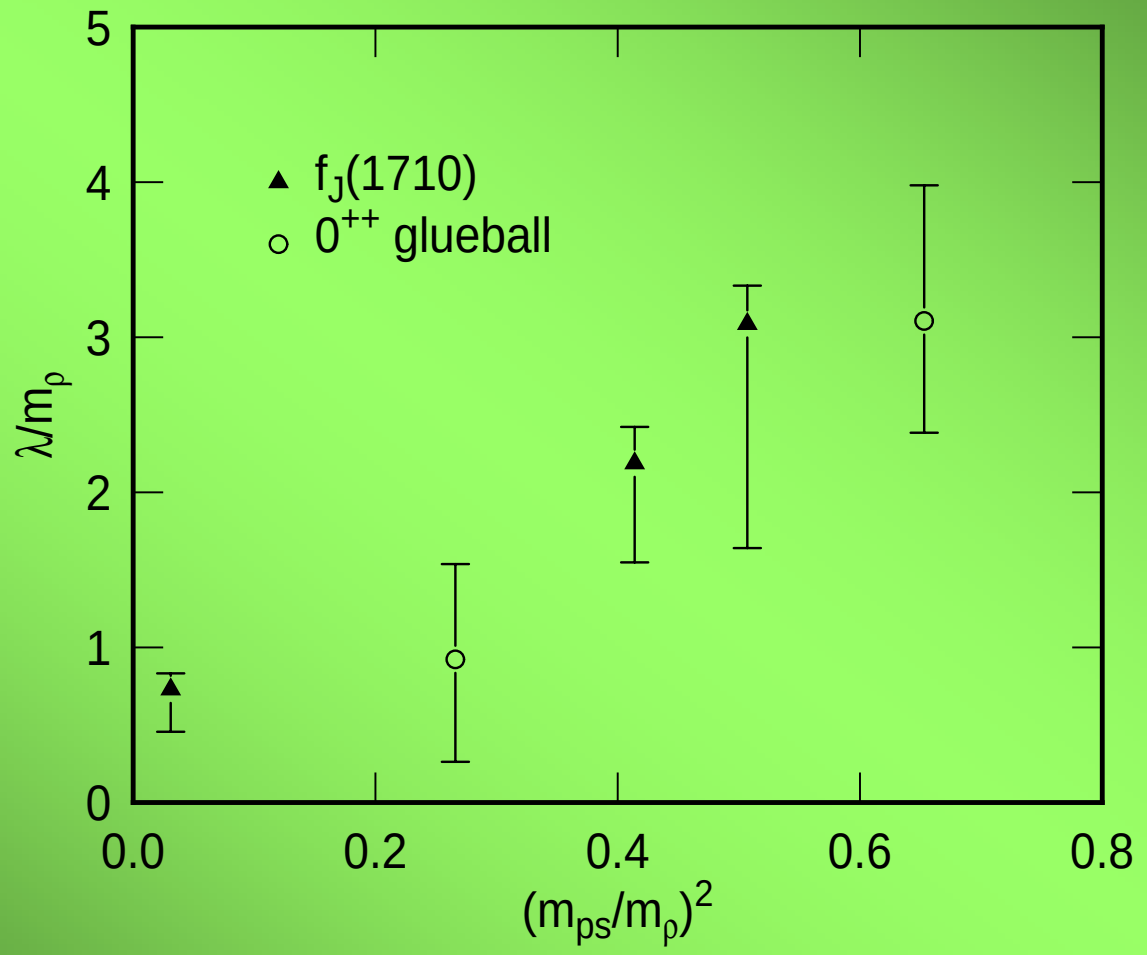

T #ghfd|v

Extracting ρ -> ππ decay couplings on the lattice

C.McNeile and C.Michael (UKQCD), PLB556, 177 (2003).

ρ –> ππ
transition

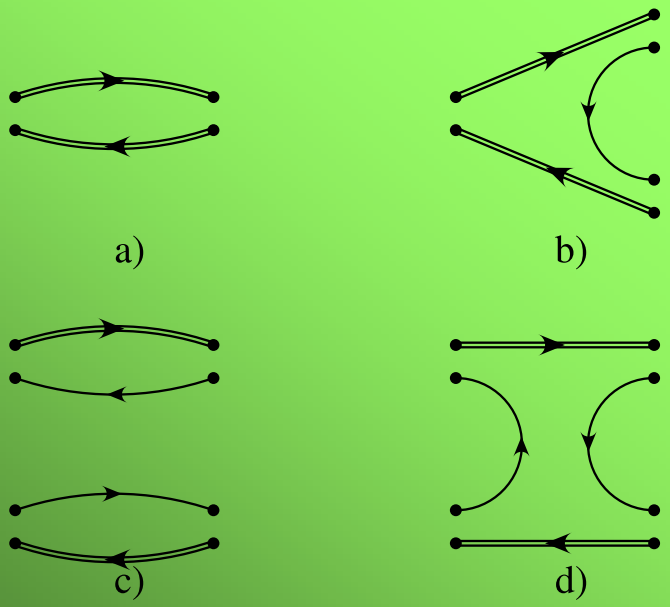

ρ –> ππ
3-pt. function

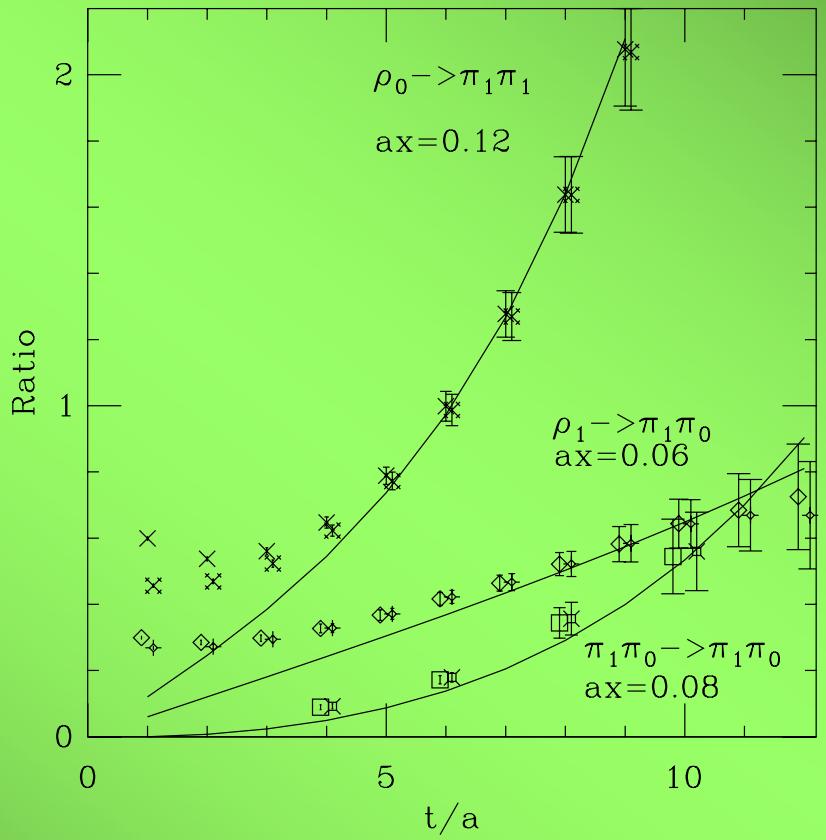

K #ghfd|v

C.McNeile, C.Michael and P.Pennanen (UKQCD), PRD65, 094505 (2002).

Very interesting prediction for experimenters:

Heavy-quark hybrids have large closed-flavor decay modes!

H -> χ+S. (estm. 61(14) MeV for b)

Suggests very nice experimental signatures, however it's a surprise, recall $\psi' \rightarrow J/\Psi\ \pi\pi$ is very small, ca. 100 keV. Needs confirmation.

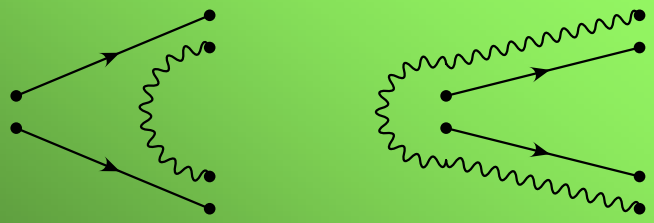

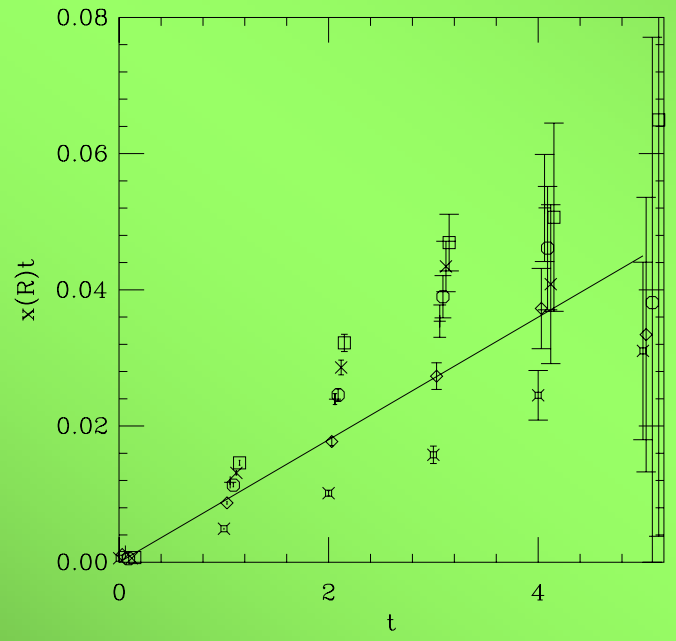


Hybrid/Exotic Mesons
Experiment

“Leading” expt. candidates for hybrid mesons (exotic and nonexotic)

state	**reported in**
$s_1(1400)$	$K\pi$
$s_1(1600)$	$u\bar{u}/d\bar{d}'$, $s\bar{s}/f_4$, b_4
$s_1(2000)$	f_4, b_4

s_2 and K_2 overpopulation (nonexotic)

others discussed include higher-mass $u\bar{d}$ and $s\bar{s}$ overpopulation

in more detail…

Hybrid mesons candidates (exotic)

$s_1(1400)$

The $k\bar{k}$ channel has a long, messy history.

It sounds like a good idea; **I =1** hence no G, no final meson spins,
all odd-L are exotic and even-L are nonexotic. "Just " extract $f_{ks}(z)$, and PWA it.

1st expt, **GAMS**, was surprised to find a nonzero exotic $ks\bar{s}$ P-wave near 1.4 GeV (weak and broad), and speculated that it was *nonresonant*.

2nd expt, **KEK**, concluded the P-wave was *resonant* but had the $a_2(1320)$ mass and width. (Feedthrough now presumed.)

3rd expt, **E852**, found a weak, broad P-wave in $ks\bar{s}^0$ near 1.4 GeV.
No consensus within the collaboration regarding it's interpretation.

4th expt, **CBarrel**, found a signal similar to E852 in pp $0A\,kss$,
and support a *resonant* interpretation.

$s_1(1400)$

$a_2(1320)$

S.U.Chung et al. (E852)
PRD60, 092001 (1999).

$s^0p \to k\#s^0p$

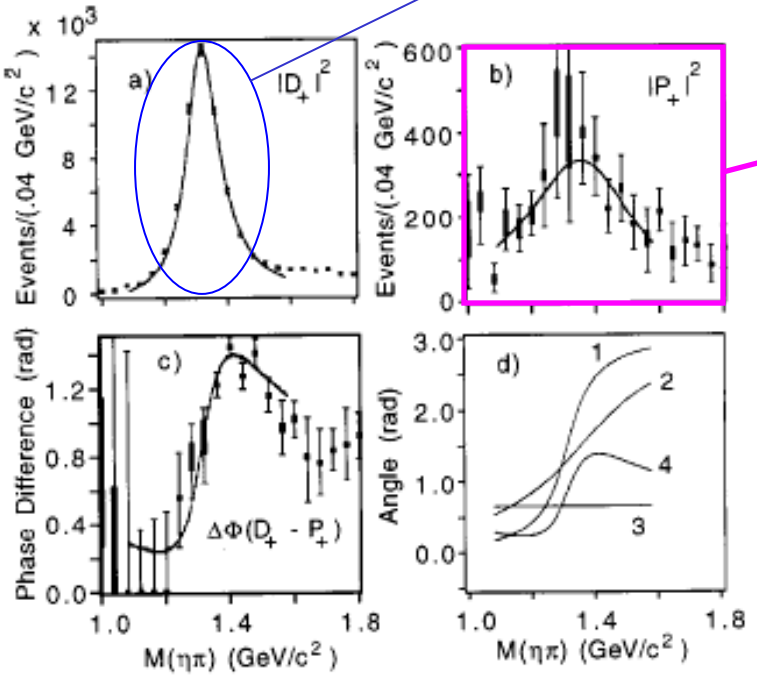

FIG. 17. Results of the partial wave amplitude analysis. Shown are (a) the fitted intensity distributions for the D_+ and (b) the P_+ partial waves, and (c) their phase difference $\Delta\Phi$. The range of values for the eight ambiguous solutions is shown by the central bar and the extent of the maximum error is shown by the error bars. Also shown as curves in (a), (b), and (c) are the results of the mass dependent analysis described in the text. The lines in (d) correspond to (1) the fitted D_+ Breit-Wigner phase, (2) the fitted P_+ Breit-Wigner phase, (3) the fitted relative production phase ϕ, and (4) the overall phase difference $\Delta\Phi$.

The famous claimed and disputed E852 broad, weak P-wave $s_{4\#}4733$, in ks^0 near 1.4 GeV.

Crystal Barrel sees a similar effect in **pp** -> kss near 1.4 GeV…
It grows curiouser and curiouser.

A.Abele et al. (CBar), PLB446, 349 (1999).

TABLE II. Comparison of the results of E852 and the Crystal Barrel for the parameters of the $J^{PC}=1^{-+}$ resonance.

	Mass (MeV/c^2)	Width (MeV/c^2)
E852	$1370\pm16^{+50}_{-30}$	$385\pm40^{+65}_{-105}$
Crystal Barrel	$1400\pm20\pm20$	$310\pm50^{+50}_{-30}$

Hybrid mesons candidates (exotic)

$s_1(1600)$

Claimed in $u\bar{u}/d\bar{d}$, $s\bar{s}$, η_4, b_4

E852

$u\bar{u}/d\bar{d}$ once a fairly strong signal, now being “revisited”.

$K^*K\pi$ is the strongest evidence for an exotic hybrid at present.

b_4 (recent result, follows).

VES

has reported mass enhancements near 1600 MeV in $u\bar{u}/d\bar{d}$, η_4

$s_1(1600)$

Possible 4^{0} exotic in $s^{0}u^{3}$

S.U.Chung et al. (E852)
PRD65, 072001 (2002).

$s^{0}p\ ^{0}A\ s\cdot s^{0}s^{0}p$

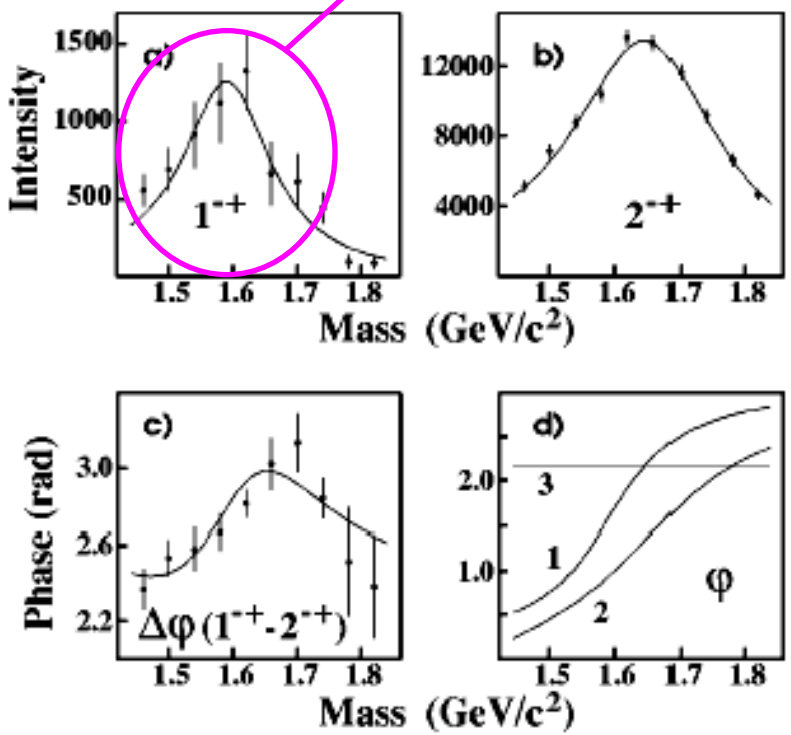

FIG. 24. A coupled mass-dependent Breit-Wigner fit of the $1^{-+}[\rho(770)]P1^{+}$ and $2^{-+}[f_2(1270)]S0^{+}$ waves. (a) $1^{-+}[\rho(770)]P1^{+}$ wave intensity. (b) $2^{-+}[f_2(1270)]S0^{+}$ wave intensity. (c) Phase difference between the $1^{-+}[\rho(770)]P1^{+}$ and $2^{-+}[f_2(1270)]S0^{+}$ waves. (d) Phase motion of the $1^{-+}[\rho(770)]P1^{+}$ wave (1), $2^{-+}[f_2(1270)]S0^{+}$ wave (2), and the production phase between them (3).

$s_1(1600)$?

A.R.Dzierba et al. (E852 Y #U)

hep-ex/0502022 10 Feb 2005

s0p 0A s·s0s0p

s0s3s3#p

No 4#0· exotic in su

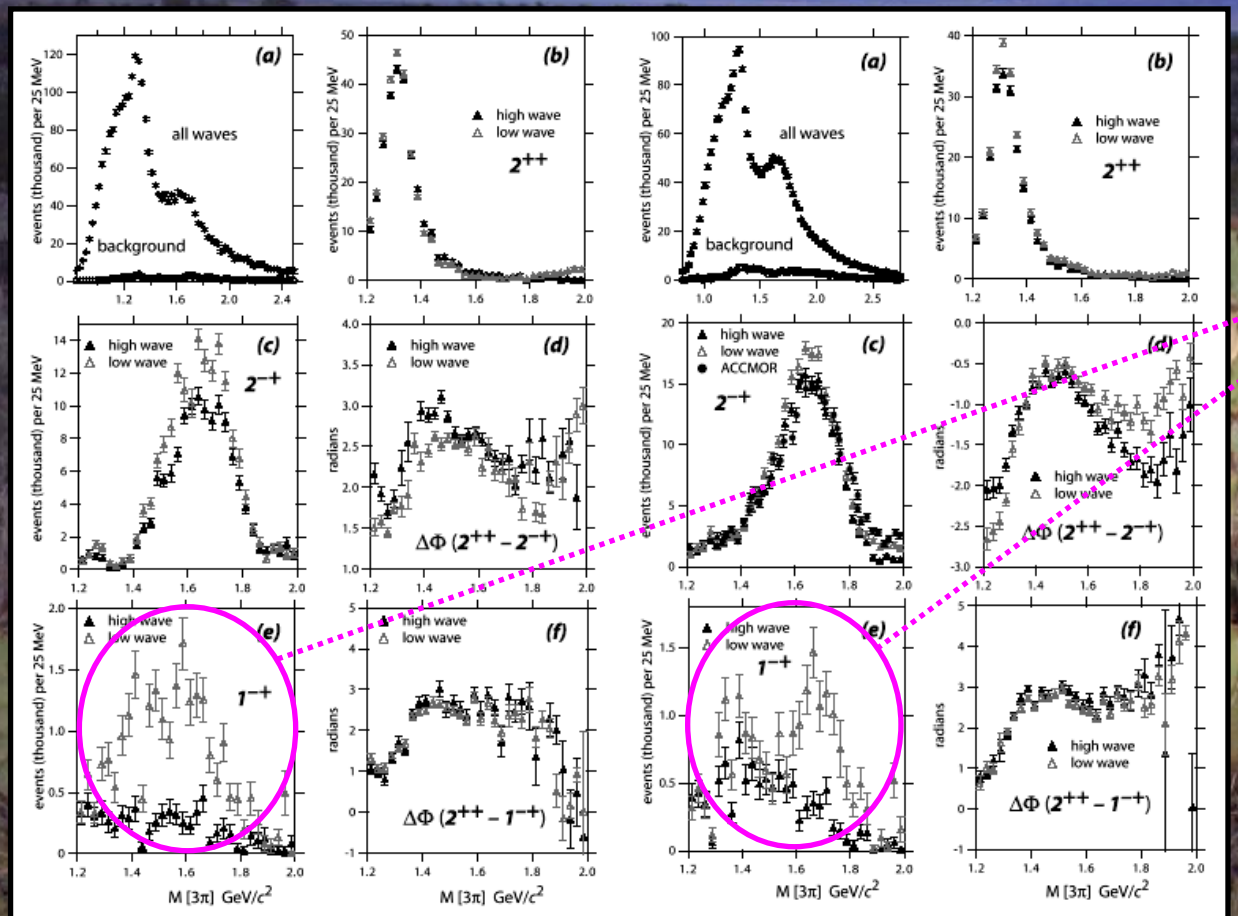

FIG. 4: PWA results for the $\pi^-\pi^0\pi^0$ channel as a function of 3π effective mass: (a) sum of all waves and the background wave; (b) 2^{++} wave; (c) 2^{-+} wave; (d) $\Delta\Phi(2^{++} - 2^{-+})$; (e) 1^{-+} wave; (f) $\Delta\Phi(2^{++} - 1^{-+})$. For (b) through (f) the results for the low wave and high wave sets are shown.

FIG. 5: PWA results for the $\pi^-\pi^-\pi^+$ channel as a function of 3π effective mass: (a) sum of all waves and the background wave; (b) 2^{++} wave; (c) 2^{-+} wave; (d) $\Delta\Phi(2^{++} - 2^{-+})$; (e) 1^{-+} wave; (f) $\Delta\Phi(2^{++} - 1^{-+})$. For (b) through (f) the results for the low wave and high wave sets are shown.

$s_1(1600)$

E.I.Ivanov et al. (E852)
PRL86, 3977 (2001).

$s^0p \to s^0k'p$

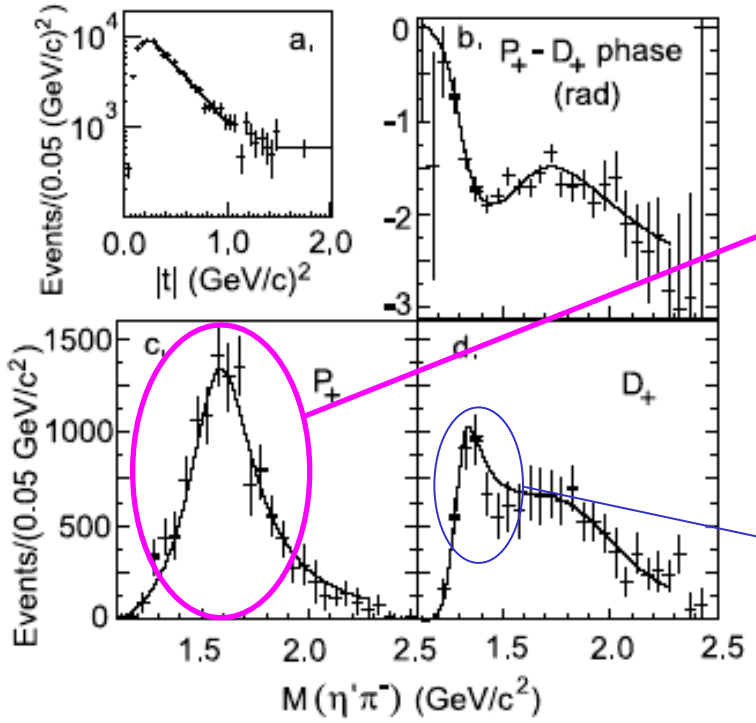

FIG. 2. (a) The acceptance-corrected $|t|$ distribution fitted with the function $f(t) = ae^{b|t|}$ (solid line). (b)–(d) The results of the mass-independent PWA (horizontal lines with error bars) and a typical mass-dependent fit (solid curve) using 0.05 GeV/c^2 mass bins. Only P_+ and D_+ partial waves and their phase difference are shown. The range of the ambiguous solutions is plotted with black rectangles. (b) The $(P_+ - D_+)$ phase difference. (c) The intensity distribution of the P_+ partial wave. (d) The intensity distribution of the D_+ partial wave. The solid curves in (b)–(d) show a mass-dependent fit (fit 1) to the P_+ and D_+ wave intensities and the $(P_+ - D_+)$ phase difference.

$s_1(1600)$
$4^{0.}$ exotic reported in s^0k'

sk' is a nice channel because nn couplings are weak for once (*e.g.* the $a_2(1320)$ noted here). The reported exotic wave is dominant!

TABLE I. Fitted resonance parameters.

Partial wave	Mass	Width
P_+	$1.597 \pm 0.010^{+0.045}_{-0.010}$	$0.340 \pm 0.040 \pm 0.050$
D_+	$1.318 \pm 0.008^{+0.003}_{-0.005}$	$0.140 \pm 0.035 \pm 0.020$
G_+	$2.000 \pm 0.040^{+0.060}_{-0.020}$	$0.350 \pm 0.100^{+0.070}_{-0.050}$

Hybrid mesons candidates (exotic)

$s_1(2000)$

Claimed in $f_4 s\bar{s}$ / $b_4 s1$ Not seen in $z u1$

E852

$f_4 s$

$b_4 s\bar{s}$ (recent result, follows).

Hybrid mesons candidates (exotic)

J.Kuhn et al. (E852)
PLB595, 109 (2004).

$\pi_1(2000)$

$\pi^0 p \to K^+ K^- \pi^0 \pi^0 p$

$f_4\pi$ (E852): higher-mass π_1 state needed to explain phase motion of the $f_4\pi$ 1^{-+} wave relative to 1^{++} and 2^{-+} waves.

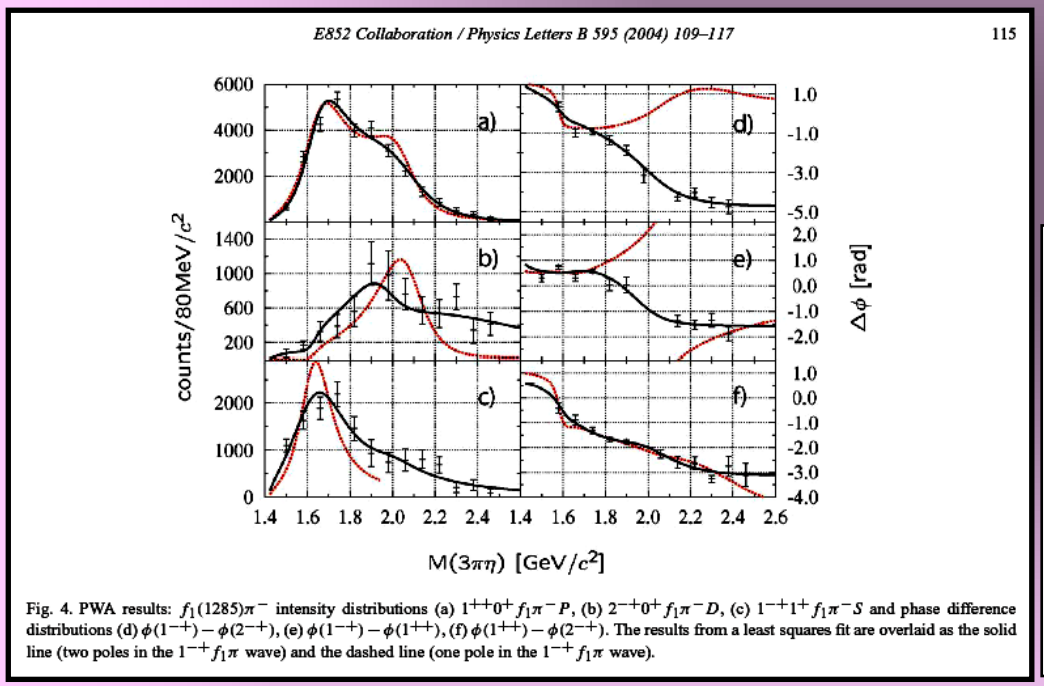

Fig. 4. PWA results: $f_1(1285)\pi^-$ intensity distributions (a) $1^{++}0^+ f_1\pi^- P$, (b) $2^{-+}0^+ f_1\pi^- D$, (c) $1^{-+}1^+ f_1\pi^- S$ and phase difference distributions (d) $\phi(1^{-+}) - \phi(2^{-+})$, (e) $\phi(1^{-+}) - \phi(1^{++})$, (f) $\phi(1^{++}) - \phi(2^{-+})$. The results from a least squares fit are overlaid as the solid line (two poles in the $1^{-+} f_1\pi$ wave) and the dashed line (one pole in the $1^{-+} f_1\pi$ wave).

Table 2
Results of the mass-dependent fit

Wave	Mass [MeV/c^2]	Γ [MeV/c^2]
$1^{++}0^+ f_1\pi P$	1714 (fixed)	308 (fixed)
	$2096 \pm 17 \pm 121$	$451 \pm 41 \pm 81$
$2^{-+}0^+ f_1\pi D$	1676 (fixed)	254 (fixed)
	$2003 \pm 88 \pm 148$	$306 \pm 132 \pm 121$
	$2460 \pm 328 \pm 263$	$1540 \pm 1214 \pm 718$
$1^{-+}1^+ f_1\pi S$	$1709 \pm 24 \pm 41$	$403 \pm 80 \pm 115$
	$2001 \pm 30 \pm 92$	$333 \pm 52 \pm 49$

No clear evidence of a $\pi_1(2000)$ in the 1^{-+} wave intensity.

Hybrid mesons candidates (nonexotic)

J.Kuhn et al. (E852)
PLB595, 109 (2004).

…and while we are here…

$s^0p\ ^0A\ k\ s\cdot s^0s^0p$

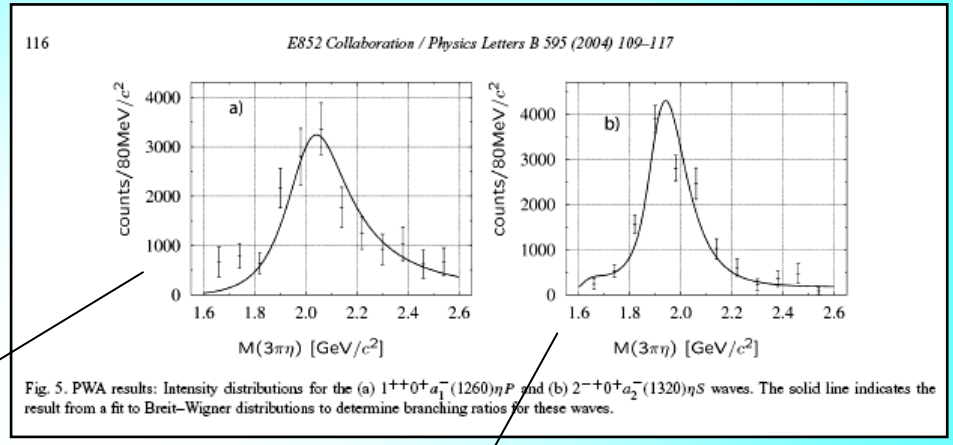

Fig. 5. PWA results: Intensity distributions for the (a) $1^{++}0^+a_1^-(1260)\eta P$ and (b) $2^{-+}0^+a_2^-(1320)\eta S$ waves. The solid line indicates the result from a fit to Breit–Wigner distributions to determine branching ratios for these waves.

In the $1^{++}0^+ f_1\pi^- P$ wave the previously observed $a_1(1700)$ is seen together with a higher lying state at 2.096 GeV/c^2. Since the $a_1(1700)$ has been interpreted as the first radial excitation of the $a_1(1260)$ [25], the $a_1(2096)$ emerges as a candidate for the second radial excitation or a hybrid meson with regular quantum numbers (*non-exotic* hybrid). The hybrid interpretation is supported by the observation of a strong decay of the $a_1(2096)$ into $a_1(1260)\eta$ in this analysis. In order to determine the relative decay ratio between these two modes the $a_1(1260)\eta$ intensity was fitted to a Breit–Wigner with the mass and width fixed at the values found in the fit of the $1^{++}0^+ f_1(1285)\pi$ wave (see Fig. 5(a)). The ratio

$$R_3 = \frac{BR[a_1(2096) \to f_1(1285)\pi]}{BR[a_1(2096) \to a_1(1260)\eta]} = 3.18 \pm 0.64 \qquad (13)$$

which is predicted to be 3 [9] if the $a_1(2096)$ is a hybrid, was determined assuming that $\rho\pi$ is the dominant decay of the $a_1(1260)$. The error quoted for

$$R_4 = \frac{BR[\pi_2(1900) \to a_2(1320)\eta]}{BR[\pi_2(1900) \to f_1(1285)\pi]} = 22.7 \pm 7.3 \qquad (14)$$

which agrees very well with the flux-tube model prediction of $R_4 = 23$ for the decay of a 2^{-+} hybrid meson at this mass [9]. Again, the error in (14) is statistical only.

[9] P.Page, E.S.Swanson and A.P.Szczepaniak, PRD59, 034016 (1999).

Hybrid mesons candidates (exotic)

M.Lu et al. (E852)
PRL94, 032003 (2005).

$s_1(2000)$

$s^0 p\ ^{0A}\ s \cdot s^0 s^0 s^3 s^3 p$

b$_4$s (E852): higher-mass s_1 state needed to explain phase motion of the ***b***$_4$s $4^{0\cdot}$ wave relative to $5^{\cdot\cdot}$ and $7^{\cdot\cdot}$ uz waves.

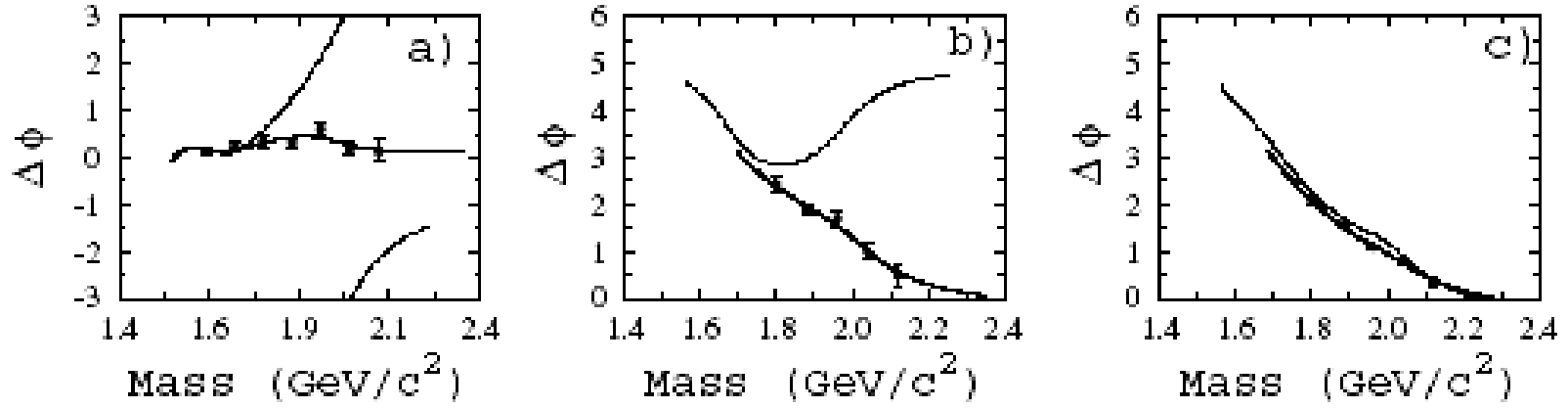

FIG. 3. Phase difference for (a) $1^{-+}(b_1\pi)_1^S 1^+ - 2^{++}(\omega\rho)_2^S 1^+$, (b) $1^{-+}(b_1\pi)_1^S 1^+ - 4^{++}(\omega\rho)_2^D 1^+$, and (c) $2^{++}(\omega\rho)_2^S 1^+ - 4^{++}(\omega\rho)_2^D 1^+$. The solid line is the Breit-Wigner result for two 1^{-+} poles and the dashed line is for one.

No clear evidence of a $s_1(2000)$ in the $1^{0\cdot}$ wave intensity.

Hybrid mesons candidates (exotic and nonexotic)

M.Lu et al (E852), PRL94, 032003 (2005).

E852: $z u^0$ and $b_1 s$

$s^0 p\ ^{0A}\ s \cdot s^0 s^0 s^3 s^3 p$

TABLE II. Resonance parameters. Here the subscript on the measured decay is the coupled intrinsic spin of the isobars.

Resonance	Decay	Mass (MeV/c^2)	Width (MeV/c^2)
$a_4(2040)$	$(\omega\rho)_2^D$	$1985 \pm 10 \pm 13$	$231 \pm 30 \pm 46$
$a_2(1700)$	$(\omega\rho)_2^S$	$1721 \pm 13 \pm 44$	$279 \pm 49 \pm 66$
$a_2(2000)$	$(\omega\rho)_2^S$	$2003 \pm 10 \pm 19$	$249 \pm 23 \pm 32$
$\pi_1(1600)$	$(b_1\pi)_1^S$	$1664 \pm 8 \pm 10$	$185 \pm 25 \pm 28$
$\pi_1(2000)$	$(b_1\pi)_1^S$	$2014 \pm 20 \pm 16$	$230 \pm 32 \pm 73$
$\pi_2(1670)$	$(\omega\rho)_{1,2}^P$	$1749 \pm 10 \pm 100$	$408 \pm 60 \pm 250$
$\pi_2(1880)$	$(\omega\rho)_{1,2}^P$	$1876 \pm 11 \pm 67$	$146 \pm 17 \pm 62$
$\pi_2(1970)$	$(\omega\rho)_{1,2}^P$	$1974 \pm 14 \pm 83$	$341 \pm 61 \pm 139$

Hybrid mesons candidates (nonexotic):

M.Lu et al (E852), PRL94, 032003 (2005).

Extra $s_2(\sim 1900)$

E852: zu^0 and $b_1 s$

$s^0 p\ ^{0A}\ s \cdot s^0 s^0 s^3 s^3 p$

Overpopulation of higher-mass s_2 states in zu^0 P-waves?

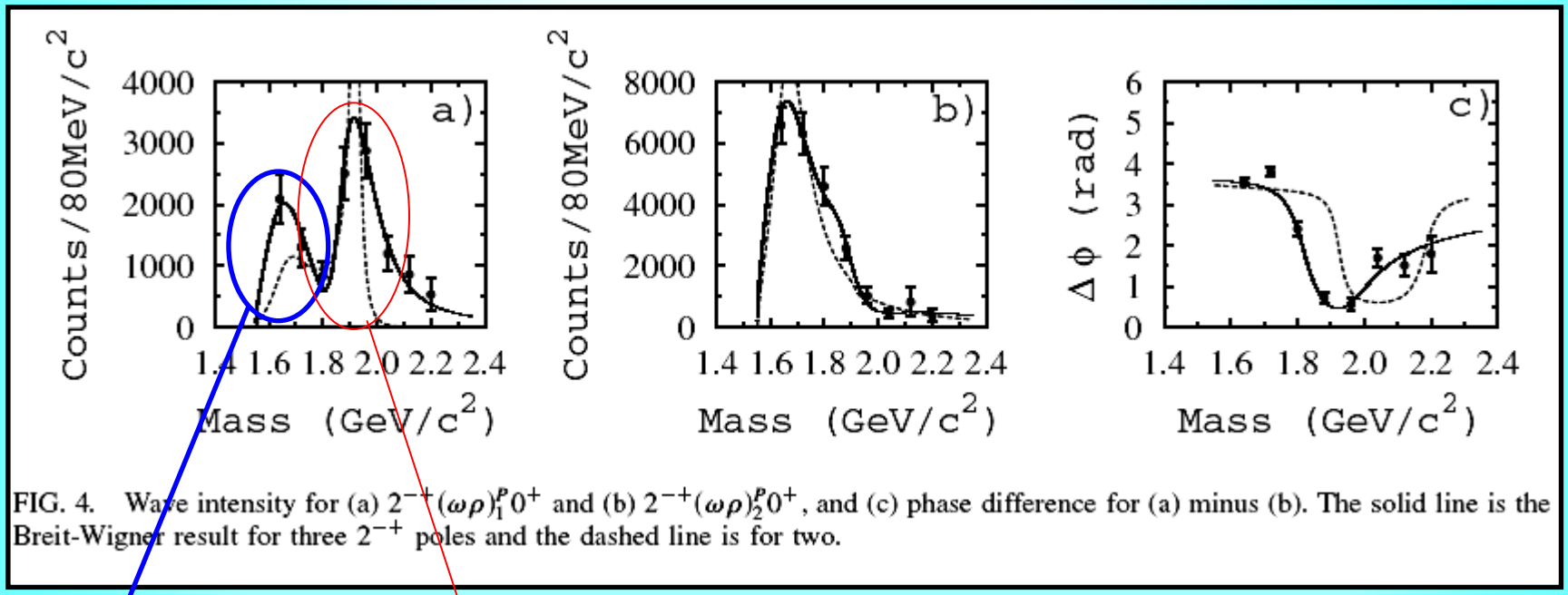

FIG. 4. Wave intensity for (a) $2^{-+}(\omega\rho)_1^P 0^+$ and (b) $2^{-+}(\omega\rho)_2^P 0^+$, and (c) phase difference for (a) minus (b). The solid line is the Breit-Wigner result for three 2^{-+} poles and the dashed line is for two.

$s_2(1670)$ $s_2(\sim 1900)$ region

Hybrid mesons candidates (nonexotic):

Extra $k_2(\sim 1850)$

J.Adomeit et al. (CBar)
ZPC71, 227 (1996).

$p\bar{p}$ ^{0A} $k s^3 s^3$

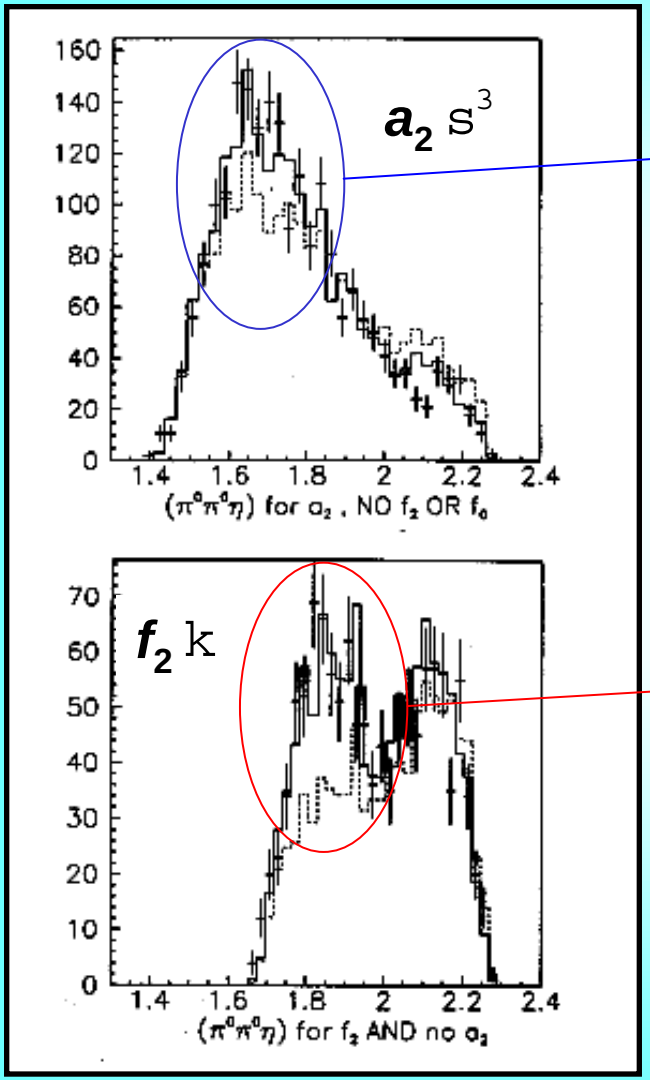

$k_2(1645)$
$n\bar{n}$ $^1D_2$ $s_2(1670)$ partner

Also evidence in jj ^{0A} $k s^3 s^3$,
central production (WA102) of
$7s$ and kss,
and now in photoproduction…

$k_2(\sim 1850)$?

Overpopulation of $n\bar{n}$ $^1D_2$ sector:
5^{0-} hybrid?

Hybrid mesons candidates (nonexotic):

Extra k_2(~1850)

T.Handler et al. (FOCUS) prelim, unpub.

jp 0A 9sX

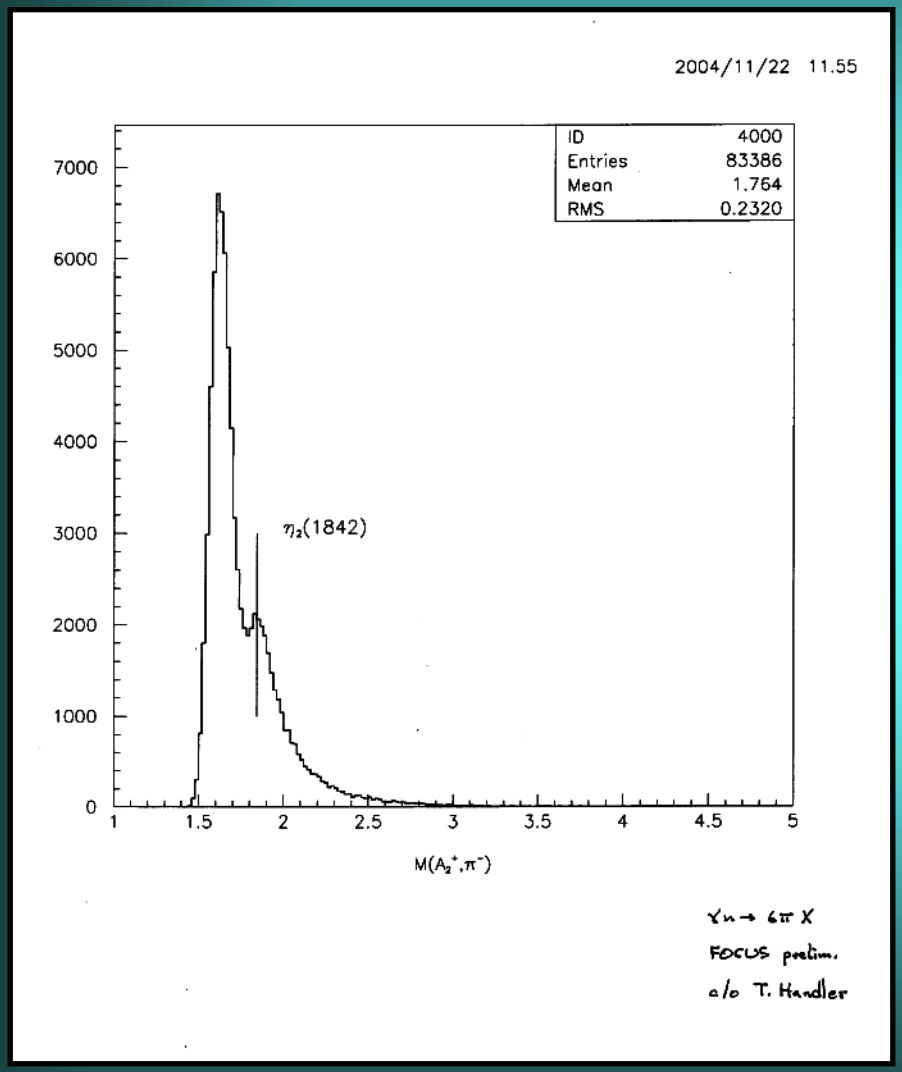

Clear higher-mass k_2 (?) peak in $a_2 \cdot s^0$ photoproduction!

…and from yesterday's discussion, $a_2 s$ is suddenly the preferred **I = 1,** $2^{\cdot 0}$ exotic-H diffractive photoproduction channel. Ù

($a_2 \cdot s^0$ has **I =1,** $2^{\cdot 0}$ as well as **I = 0,** $2^{0\cdot}$)

Hybrid mesons candidates (nonexotic):

Extra k_2(~1850)

Table S11. 1^1D_2 (*alt.*)		
	$\eta_2(1842) = s\|n\bar{n}\rangle + c\|s\bar{s}\rangle$	
Mode	Γ_i(MeV)	Amps.
KK^*	$111.7c^2 + 158.0sc + 55.9s^2$	$^3P_2 = -0.116c - 0.0820s$ $^3F_2 = -0.0580c - 0.0410s$
K^*K^*	$12.1c^2 - 17.1sc + 6.1s^2$	$^3P_2 = -0.10$ $^3F_2 = +0.00506c - 0.00358s$
$KK_1(1273)$	$0.2c^2 - 0.3sc + 0.1s^2$	$^3D_2 = +0.00977c - 0.00691s$
$\rho\rho$	$129.9s^2$	$^3P_2 = +0.231s$ $^3F_2 = -0.0765s$
$\omega\omega$	$40.3s^2$	$^3P_2 = -0.229s$ $^3F_2 = -0.0689s$
πa_1	$33.8s^2$	$^3D_2 = +0.0986s$
ηf_1	0.0	$^3D_2 = -0.00321s$
$\pi a_0(1450)$	$0.6s^2$	$^1D_2 = +0.0182s$
πa_2	$260.7s^2$	$^5S_2 = +0.285s$ $^5D_2 = +0.109s$ $^5G_2 = +0.00681s$
ηf_2	$30.0s^2$	$^5S_2 = -0.314s$ $^5D_2 = -0.00721s$ $^5G_2 = -0.0000358s$
	$\Gamma_{thy} = 141c^2 + 124sc + 557s^2$ MeV	
	$\Gamma_{expt} = 225 \pm 14$ MeV	

Could this k_2 instead be evidence for Zweig mixing in the 2^{0^-} sector?

$|k_2\rangle = s|n\bar{n}\rangle + c|s\bar{s}\rangle$?

This can be tested: relative BFs and decay amplitudes for flavor-mixed $q\bar{q}$ k_2 states have been calculated.

PRD68, 054014 (2003).

n.b. Mixed $q\bar{q}$ doesn't work, it predicts $f_2^k << a_2^s$.

Surv Itdnl$

Flavor-tagging J/| 0A V f hadronic decays, an e.g.:

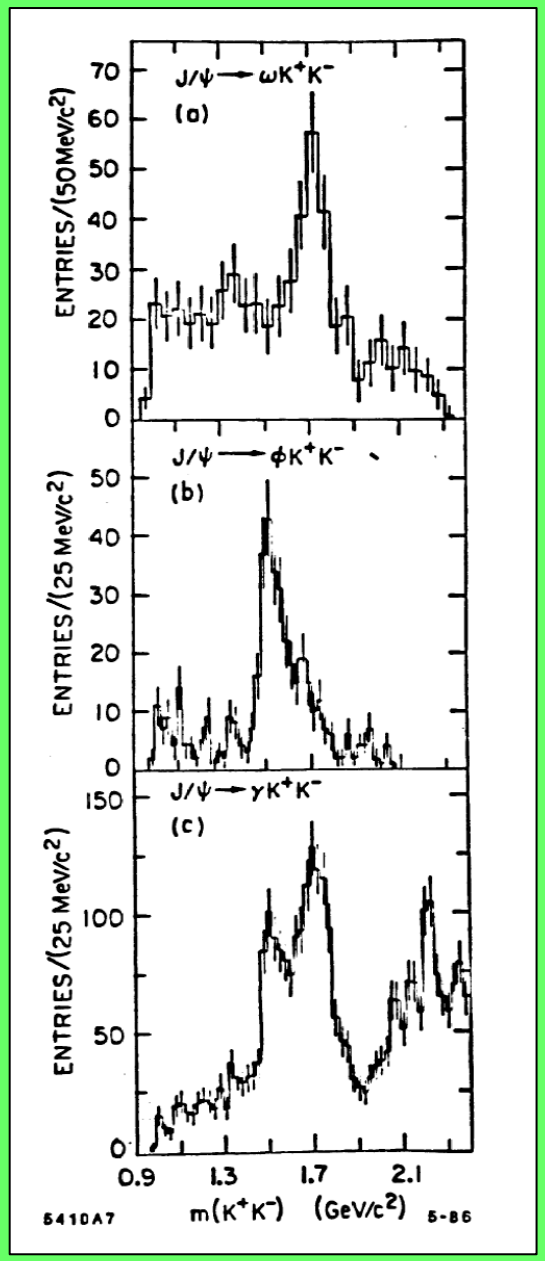

J.J.Becker et al. (MarkIII)
SLAC-PUB-4243 (Feb.1987)

Against z , you see the $f_0(1710)$.
No $f_2'(1525)$ (ss).

Against i, you see the $f_2'(1525)$ (ss).
Weak $f_0(1710)$ shoulder claimed.

Against j you see both.
No nn/ss flavor discrimination.

DEAR CLEO, PLEASE DON'T FORGET:


Hybrid Baryons

Spectrum of light (n=u,d) |nnng> + … hybrid baryons.

Several bag model calculations, early/mid 1980s.
T.Barnes and F.E.Close, PLB123, 89 (1983) (shown),
E.Golowich, E.Haqq and G.Karl. Phys.Rev.D28, 160 (1983), err.D33, 859 (1986).
C.E.Carlson, T.H.Hansson and C.Peterson, PRD27, 1556 (1983).

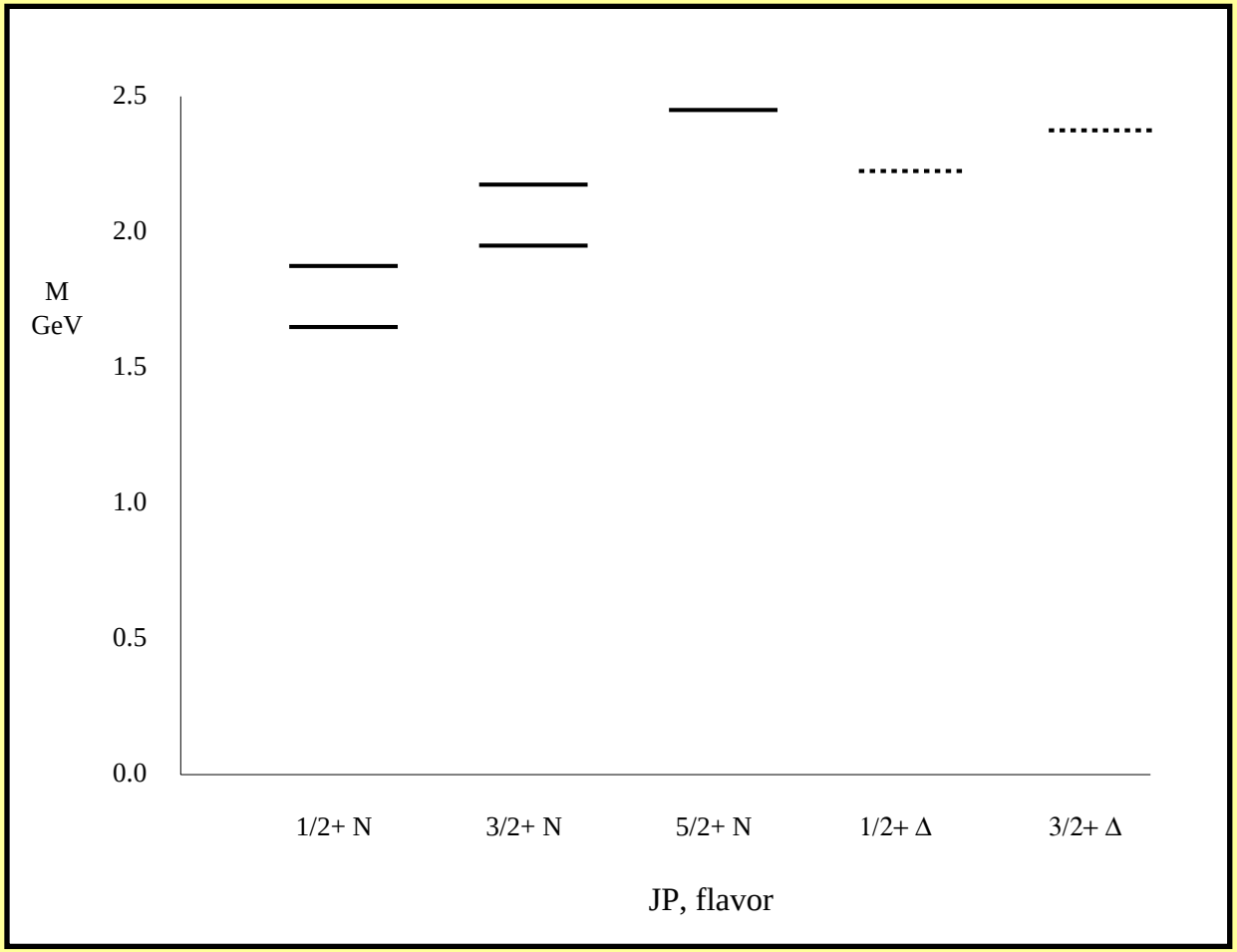

Spectrum of light (n=u,d) hybrid baryons.

S.Capstick and P.R.Page,
nucl-th/0207027, Phys. Rev. C66 (2002) 065204.

(flux tube model)

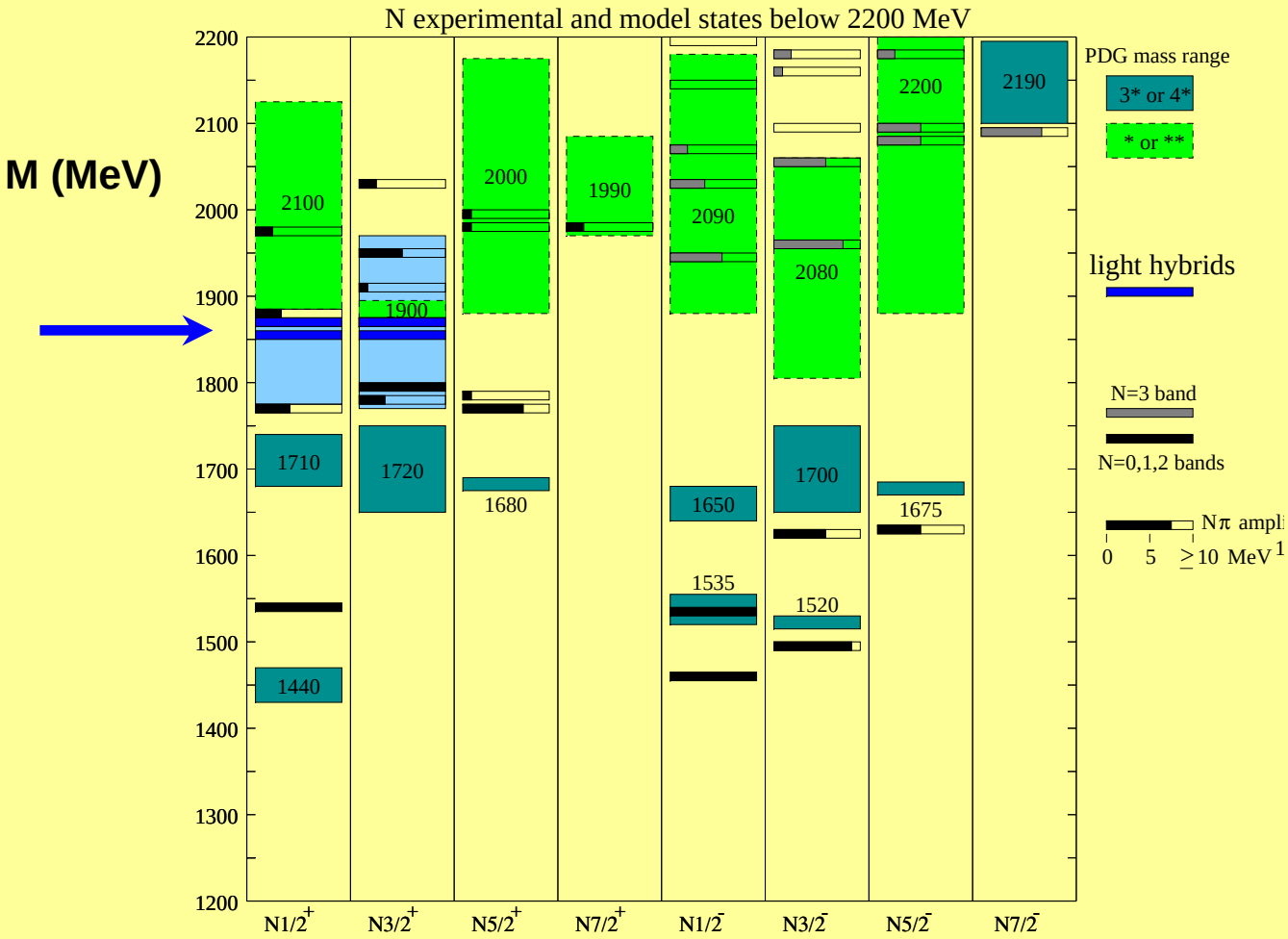


…waiting for the dawn.
J/| 0A j f, V f
|′0A j f, V f
j 0A f

Table 1
List of waves used in the final PWA fit

$J^{PC}m^{\epsilon}$	Primary decay	L	S	# of waves
$0^{-+}0^{-}$	$\eta(1295)\pi^{-}$	0	0	2
$0^{-+}0^{-}$	$a_0^{-}(980)\sigma$	1	0	1
$2^{++}0^{-}$	$a_2^{-}(1320)\sigma$	0	2	1
$2^{++}0^{-}$	$a_2^{-}(1320)\rho$	1, 3	1, 2, 3	6
$1^{-+}1^{+}$	$a_0^{-}(980)\rho$	0	1	1
$1^{-+}1^{+}$	$a_1^{-}(1260)\eta$	0	1	2
$1^{-+}1^{+}$	$f_1(1285)\pi^{-}$	0	1	2
$1^{-+}1^{+}$	$\rho'(1460)\pi^{-}$	1	1	1
$1^{++}0^{+}$	$a_0^{-}(980)\rho$	1	1	1
$1^{++}0^{+}$	$a_1^{-}(1260)\eta$	1	1	2
$1^{++}0^{+}$	$f_1(1285)\pi^{-}$	1	1	2
$1^{++}0^{+}$	$a_2^{-}(1320)\eta$	1	2	1
$1^{++}0^{+}$	$\rho'(1460)\pi^{-}$	0, 2	1	2
$1^{++}0^{+}$	$\rho_3(1690)\pi^{-}$	2	3	1
$2^{-+}0^{+}$	$a_2^{-}(1320)\eta$	0	2	1
$2^{-+}0^{+}$	$\rho'(1460)\pi^{-}$	1	1	1
$2^{-+}0^{+}$	$a_1^{-}(1260)\eta$	2	1	2
$2^{-+}0^{+}$	$f_1(1285)\pi^{-}$	2	1	2
$2^{++}1^{+}$	$\pi_2^{-}(1670)\eta$	0	2	2
$2^{++}1^{+}$	$a_2^{-}(1320)\rho$	1	1, 2, 3	3
$2^{++}1^{+}$	$a_2^{-}(1320)\eta$	1	2	1
$3^{++}0^{+}$	$a_2^{-}(1320)\eta$	1	2	1
$3^{++}0, 1^{+}$	$a_2^{-}(1320)\rho$	1	2, 3	4
$3^{++}0^{+}$	$a_1^{-}(1260)\eta$	3	1	2
$4^{++}1^{+}$	$a_2^{-}(1320)\rho$	1	3	1
$4^{++}1^{+}$	$a_2^{-}(1320)\rho$	3	1, 2, 3	3
$4^{++}1^{+}$	$a_1^{-}(1260)\eta$	3	1	2
$4^{++}1^{+}$	$a_2^{-}(1320)\eta$	1	2	1
$4^{++}1^{+}$	$\pi^{-}(1800)\eta$	4	0	2
Background				1